AFRICA CENTRE OF EXCELLENCE FOR WATER MANAGEMENT

ADDIS ABABA UNIVERSITY

COLLEGE OF NATURAL AND COMPUTATIONAL SCIENCES

SCHOOL OF GRADUATE STUDIES

DEPARTMENT OF HYDROLOGY AND WATER RESOURCES

M.Sc. Thesis

Peak flow Projections under the Influence of Climate Change: impact and uncertainty evaluation in the Upper Awash River Basin, Ethiopia

By

Tarikua Berhane Abreha

Supervisor: Dr. Hadush Kidane Meresa

September 2021 Addis Ababa – Ethiopia

APPROVAL PAGE

Peak flow Projections under the Influence of Climate Change: impact and uncertainty evaluation in the Upper Awash River Basin, Ethiopia

BY

Tarikua Berehane

The thesis entitled "Peak flow Projections under the Influence of Climate Change: impact and uncertainty evaluation in the Upper Awash River Basin, Ethiopia" by Tarikua Berhane is approved for the degree of Master of Science in Hydrology and water resource management.

Approved by Board of Examiners

Dr. Hadush Kidane Meresa	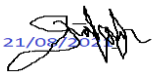	_____
Advisor	Signature	Date
Dr. Dessie Nedaw	_____	_____
Internal Examiner	Signature	Date
Dr. Sirak Tekleab	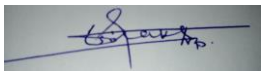	_____
External Examiner	Signature	Date
Dr. Getachew Dagnew	_____	_____
Chairman	Signature	Date

Declaration

This thesis entitled “Peak flow Projections under the Influence of Climate Change: impact and uncertainty evaluation in the Upper Awash River Basin, Ethiopia” is my original work and has been not presented or published for a degree in other universities and that all sources of materials used in this thesis work are duly acknowledged.

Tarikua Berhane Abreha _____

ACKNOWLEDGMENT

First of all, I would like to thank the almighty God for giving me the strength to walk unpaved way to reach this point in life.

I would like to express my appreciation to my employer and sponsor, Arba Minch University for the offer of chance to pursue my MSc study. Also I would like to express my deepest appreciation and heartfelt thanks to Addis Ababa University staffs who gave their time so generously.

Furthermore, I would like to convey a heartfelt gratitude to my beloved families specially my mom Kaleyta Belay without your prayer I could not be here. My special heartfelt gratitude also goes to my husband Alazar Getachew for his valuable advice, support, encouragement, quiet patience and unspeakable loves were the driving force for all achievements I have been earning.

Finally, and most importantly, I would like to thank my Classmate and friends Rediet B., Betelhem S., Eyerusalem B., Tsigabu K, Emebet D., Yeshiemebet S., Ephrem, Tilaye W., Assebe A., Aster Abel, Abdissa S., Mendy and others for their encouragement, moral support and true friendship we shared all the fun and sorrow during my stay in Addis it means a lot to me.

ABSTRACT

Modelling climate change impact on peak flood is subject to considerable uncertainty that comes from the climate model discrepancies, climate bias correction methods, and hydrological model parameters. These factors play a crucial role in flood risk planning and extreme event management. With the advent of the Coupled Model Inter comparison Project Phase 6 (CMIP6), flood managers and water resource planners are interested to know changes in catchment flood risk are expected to alter relative to previous assessments. A catchment-based projected change in peak flood quantiles for Upper Awash catchment was quantified. Conceptual hydrological model, three downscaling techniques, and an ensemble of hydrological parameter sets were used to examine changes in peak flood quantile magnitude and frequency under climate change in the mid and end of the 21st century. The results show that projected annual extreme precipitation and peak flood quantiles could increase substantially in the coming decades by 30%-55% in all the selected catchments. The associated uncertainty in future peak flood quantiles was quantified using aggregated variance decomposition and the result confirms that climate change is the dominant factor in Akaki (55%) and Awash H (51%) catchments, whereas the bias correction approaches in Awash B (58%) and Kela (50%) catchments. In Awash catchment both climate models and bias correction methods (45% and 49%, respectively) are the most dominate factors in projected peak flood magnitude. The hydrological parameter sets are identified as least important factor in the flood projections. Moreover, these results may add some significant information in the range of plausible changes expected for policy-relevant flood indices, and the tailoring of adaptation plans to account for the new generation climate model outputs.

Keywords: CMIP6, HBV, bias correction, hydrology, extremes

TABLE OF CONTENTS

Contents Pages
ACKNOWLEDGMENT I
ABSTRACT IV
TABLE OF CONTENTS V
LIST OF FIGURES 1
LIST OF TABLES 3
ABBRIVATIONS 4
1. INTRODUCTION 6
1.1 Background 6
1.2 Statement of the problem 8
1.3 Research Objectives 9
1.3.1 General Objective 9
1.3.2 Specific Objectives 10
1.4 Research Questions 10
1.5 Significance of the study 10
1.6 Scope of the study 10
1.7 Novelty/ Contribution of the study 11
2. LITERATURE REVIEW 12
2.1 Climate Change 12
2.1.1 Causes of Climate Changes 13
2.1.2 Climate Change in Ethiopia 13
2.1.3 Impact of climate change in Upper Awash River Basin 13
2.2 Modeling Climate Change 14
2.2.1 Climate Change Scenarios 15
2.2.2 Downscaling Methods and Tools 16
2.2.3 Methods of Bias Correction 17
2.2.4 Coupled Model Intercomparison Project (CMIP 6) Data in Africa 18
2.3 Hydrological Extremes and climate Change 19
2.4 Hydrological Modelling 20
2.4.1 Hydrological Model Selection Criteria 21
2.4.2 The HBV model 22
2.4.3 Why the model was selected 22

2.5 Researchable Issues in using HBV Model 23
2.6 Related Studies in Ethiopia 24
3. DESCRIPTION OF THE STUDY AREA 25
3.1 Location 25
3.2 Climatic condition 26
3.3 Land use and soil type 26
3.4 Datasets 27
3.4.1 Historical Hydro-Meteorological Data 28
3.4.2 Future data 29
3.5 Data availability 29
4. METHODS 31
4.1 Data Processing and Analysis 31
4.1.1 Filling Missing data 31
4.1.2 Homogeneity and consistency test 31
4.1.3 Potential evapotranspiration (PET) 33
4.2 Bias correction techniques 33
4.2.1 Statistical quantile factor change (SQF) 34
4.2.2 Distribution Quantile Mapping (DQM) 34
4.2.3 Empirical quantile mapping (EQM) 35
4.3 Bias correction performance evaluation 35
4.4 Coupled Model Intercomparison Project phase 6 (CMIP6) 36
4.5 Hydrological modelling 37
4.5.1 Hydrological model parameter selection and evaluation 39
4.6 Flood frequency analysis 39
4.7 Generalized Likelihood Uncertainty Estimation (GLUE) 40
4.8 Uncertainty decomposition and estimation 41
4.9 Research Flow Chart 42
5. RESULT AND DISCUSSIONS 43
5.1 Evaluation and validation of different climate bias correction techniques 43
5.2 Hydrological modeling and parameter uncertainty evaluation 46
5.3 Performance of hydrological models under different bias correction approach 49
5.4 Flood quantile projections under varying climate conditions 50
5.5 Uncertainty estimation and decomposition of associated sources in flood quantile estimation 51

5.6 Discussion 53
5.6.1Projected hydro climatic variables using CMIP6 scenarios 53
5.6.2 Modelling and projections of hydrological extremes using CMIP6 dataset 54
5.6.3 Flood quantile estimation under climate change 55
5.6.4 Projected Flood quantile associated Uncertainty estimation and decomposition 56
6. CONCLUSIONS AND RECOMMENDATIONS 59
6.1 Conclusions 59
6.2 Recommendation 60
REFERENCES 61
APPENDICES 75
Appendices - A1: Filling in missed rainfall and temperature data 75
Appendices - A2: Rainfall data-set consistency test methodology 75

LIST OF FIGURES

Figure 3.1 Location map of the study area 26

Figure 3.2 Soil type and LULC of UAB.....27

Figure 3.3 Location of hydro-meteorological Stations and Digital Elevation model of UARB 29

Figure 4.1 Homogeneity test of rainfall stations of UAB.....32

Figure 4.2 Double mass curve of rainfall data.....33

Figure 4.3 Hydrologiska Byråns Vattenbalansavdelning (HBV) hydrological model structure (Bergström, 1981)……...39

Figure 4.4 Research flow chart to estimate projections of flood quantile and identify associated uncertainty……..43

Figure 5.1Comparison of three bias correction techniques with observed daily maximum precipitation using a statistical matrix. The column represents each catchment using three bias correction methods, and each row represents each climate model. S1 stands for Awash Koka, S2 Akaki, S3 Kela, S4 Awash Bello, and S5 Awash Hombole. 43

Figure 5.2 Comparison of seasonal raw and bias corrected daily maximum precipitation simulations from 12 CMIP6 GCMs for each of five study catchments. Each column presents results of one bias correction method of five catchments. Each row presents a result of three bias correction methods of one catchment. In each panel the shaded area represents the range of 12 GCMs, and blue line is the raw median of raw 12 GCMs with black line the observed seasonal maximum precipitation. S1 stands for Awash Koka, S2 Akaki, S3 Kela, S4 Awash Bello, and S5 Awash Hombole. 45

Figure 5.3 Ensemble of 12 climate models of mean air temperature projections for the period 1975-2100. The orange, Blue, and Green shaded areas stand for the spread of SSP585, SSP370, and SSP126 scenarios, respectively. The solid lines represent the 12 climate models' median for each scenario – red for SSP5, blue for SSP3, and SSP1. 46

Figure 5.4 HBV hydrological model performance in the calibration period using the NSE objective function**.** .....**Error! Bookmark not defined.**

Figure 5.5 HBV hydrological model performance in the validation period using the NSE objective function. .....**Error! Bookmark not defined.**

Figure 5.6 River flow change in clim1 (2010-2039), clim2 (2040-2069), and clim3 (2071-2100) with respect to the reference period (1981-2010). Each box plot represents the spread of twelve

climate models listed in Table 4.3 with median 0.5 and 0.25 and 0.75 quantiles. Each column stands for each scenario (the first column for SSP126, the second column for SSP370, and the third column for SSP585). Each row represents each catchment (first row S1- Awash Koka, second row S2- Akaki, third row S3- Kela, fourth row S4- Awash Bello, and the last row for S5- Awash Hombole). The red box at the top of the both in the right side indicates extreme outlier points..... **Error! Bookmark not defined.**

Figure 5.7 Changes in peak flow quantiles using three bias correction techniques and GEV frequency distribution model at each catchment. First column (climate inputs with EQM correction; second row) climate inputs with DQM correction; and third row) climate inputs with SQF correction. S1 stands for Awash Koka, S2 Akaki, S3 Kela, S4 Awash Bello, and S5 Awash Hombole.....**Error! Bookmark not defined.**

Figure 5.8 Contribution of each source of uncertainty in flood frequency estimation under climate change. The three circles present flood quantile results at RT=20 yrs, RT=50 yrs, RT=100 yrs from inside to outside, respectively. Each color represents each source of uncertainty: dark green is uncertainty from climate models (CC), light green from bias correction methods (BC), and Blue color from hydrological parameters (HP), and the other colors represent the interaction between the main factors.....**Error! Bookmark not defined.**

LIST OF TABLES

Table 2.1 Shared socio-economic pathway (SSPs)..... 16
Table 3.1 Data sets used in the study..... 28
Table 3.2Meteorological stations used in the study..... 29
Table 3.3 Statistical description of the five selected gauged stations..... 30
Table 4.1 List of climate models used in this study..... 37
Table 4.2 A range of hydrological parameters of HBV model..... 39
Table 5.1 Optimal parameters of HBV hydrological model using NSE objective function……..49

ABBRIVATIONS

ANOVA - Analysis of Variance

BCM - Billion Cubic Meter

CORDEX - Coordinated Regional Downscaling Experiment

CMIP - Coupled Model Intercomparison Project

DEM - Digital Elevation Model

DMC - Double Mass Curve

DQM - Distribution Quantile Mapping

EMA - Ethiopian Mapping Agency

EQM - Empirical Quantile Mapping

GCMs - Global Climate Models

GEV - Generalized Extreme Value

GLUE - Generalized Likelihood Uncertainty Estimation

HBV - Hydrologiska Byråns Vattenbalansavdelning

HEC-HMS - Hydrologic Engineering Center-Hydrologic Modeling System

HSPF - Hydrologic Simulation Program-Fortran

IHMS - Integrated Hydrological Modelling System

IPPC - Intergovernmental Panel on Climate Change

ITCZ - Inter Tropical Convergence Zone

KW - Kinematic Wave

LULC - Land Use Land Cover

MAE - Mean Absolute Error

MOWIE - Ministry of Water, Irrigation and Electricity

NARF - Normal Annual Rainfall

NMSA - National Meteorological Service Agency

NSE - Nash-Sutcliffe

PDM - Probability Distributed Models

PDF - Probability Density Function

PET - Potential Evapotranspiration

PPM - Parts Per Million

RCMs - Regional Climate Models

RMSE - Root Mean Square Error

SD - Statistical Downscaling

SDSM - Statistical Down-Scaling Model

SRTM - Shuttle Radar Topographical Mission

SRES - Series Report Emission Scenarios

SSP - Shared Socioeconomic Pathways

SQF - Statistical Quantile Factor Change

UAB - Upper Awash River basin

VIC - Variable Infiltration Capacity

WCRP - World Climate Research Program

1. INTRODUCTION

1.1 Background

In the coming decades, climate change will likely become a primary problem affecting hydrological regimes and water resource availability conditions. Significant changes in atmospheric temperature, precipitation, humidity, and circulation are expected, resulting in increased extreme events, including floods, droughts, heatwaves, heavy rainfall, and more intense cyclones (Knutti & Sedláček, 2013; IPPC, 2013).

Similarly, Serdeczny et al., 2016 and Rojas et al., 2013, also stated that the extreme peak frequency will be increased due to climate change, and has a massive impact on the socio-economic status of the region. African flood magnitude, frequency, pattern, and timing are shifting due to climate change, and its consequences are not uniform across the region. In Ethiopia, summer peak flows are significantly increasing due to climate change. This increase in peak flow magnitude is due to increasing future precipitation, to a large positive change in rainfall intensity and frequent during the summer season (Serdeczny et al., 2016).

In contrast, increasing air temperature in the autumn and winter seasons lead to increase drought magnitude due to increasing evapotranspiration (Coulibaly et al., 2020;Thober et al., 2018;Balke & Nilsson, 2019;Blöschl et al., 2019). Understanding of catchment-scale flood quantile projections is crucial for water resource planning and flood risk management. However, it is challenging to quantify the impact at different modeling stage that possess, downscaling the GCMs/RCMs output to catchment scale, and projection of hydrological extremes using the bias-corrected climate variables, and estimate the impact of climate change on design flow values at different return period, and quantify the associated uncertainty. Therefore, it is important to improve the peak flow simulations and estimate their respective role on flood design values at different return period.

Similarly, the impact of climate change on the local hydrological extremes are uncertain, complicated, extensive, and interrelated, propagated from the global coarse resolution scale to the local scale (Joseph et al., 2018; Wang et al., 2019; Osman et al., 2019; Byun et al., 2019; Wang et al., 2019; Gao et al., 2020; Her et al., 2019; Hattermann et al., 2018).

Meresa and Romanowicz, 2016, studied the critical uncertainty embedded (hydrological parameter uncertainty (HBV), climate models (representative concentration pathway (RCP)), and distribution

parameter uncertainty (Generalized extreme value (GEV))) in the projection of hydrological extremes and addressed that regional impact study is highly prone to climate models chain error. Joseph et al., 2018 also considered hydrological parameters (variable infiltration capacity (VIC)) and climate models (RCP) uncertainty assessment in seasonal flow projections. Evaluated the uncertainty of bias correction methods on flood frequency and found that the climate models biases had significant change in the magnitude of flood design values. Therefore, the changes in peak flow due to discrepancies of climate model's evaluation are associated with various uncertainty sources.

The main uncertainty components in coupling of climate models to hydrological model for local impact assessment are associated with climate models, hydrological parameters, downscaling/bias correction approaches, and flood frequency model types (Bastola et al., 2011;Meresa and Romanowicz, 2017;Charles et al., 2019; Meresa, 2019;Lawrence, 2020). Therefore, it is crucial to estimate and understand the complex and uncertain impact and challenge identifying the main sources of uncertainty in future quantile estimation and future flood risk and extreme management.

In the last decades, multiple types of climate scenarios (series report emission scenarios (SRES), representative concentration pathway (CORDEX), shared socio-economic pathway (CMIP)) with several regional climate models/global climate models (RCMs/GCMs) have been deployed with different atmospheric-land physical formulations, hence giving a wide range of climate model outputs. Therefore, the projected hydrological extremes at local scale are highly dependent on the spreads of RCMs/GCMs employed (Woldemeskel et al., 2014; Meresa and Romanowicz, 2017;Hattermann et al., 2018;Charles et al., 2019; Meresa, 2019;Lawrence, 2020).

The information from multiple GCMs/RCMs spreads are considered as uncertainty; and can be quantified using the variance of the climate models (Meresa and Romanowicz, 2017; Lawrence, 2020), imprecise probability (Aven, 2019), probabilistic combination technique (Das, et al,2018), the variance of the error between the observed and each climate model approach. These studies mainly focused on the uncertainty of climate model interpretation and not emphasizing its other factors (e.g. downscaling). Bias correction methods have a significant impact on the projected hydrological extremes, magnitude, and direction (Pierce et al., 2015;Hattermann et al., 2018;Charles et al., 2019). Nowadays, many researchers have been used and addressed the importance of climate bias correction methods (Kay et al., 2009; Saini et al., 2015;).

Quantile mapping, empirical mapping, simple statistical transformation, and joint probability are most popular and widely applied for climate model bias correction. These techniques will reduce the original climate model variability and outliers for forcing hydrological models. The major source of uncertainty in climate projection could be explained by selecting bias correction methods and the spread of selected GCMs.

Besides to climate model variance and reliability of climate model's bias correction techniques, it is also a challenge to obtain the most representative hydrological model parameters sets in space and time. In the projection of hydrological extremes, the combination of the hydrological parameters plays a major role in minimizing the uncertainty related to catchment hydrological (Pechlivanidis et al., 2017;Joseph et al., 2018;Her et al., 2019). Many studies attempt to address the uncertainty of the hydrological parameters in climate change impact study using GLUE (generalized likelihood uncertainty estimation) (Beven & Binley, 1992), multi-objective function optimization approach (Dakhlaoui et al., 2017;Zhang et al., 2019), Bayesian Model Averaging (Beigi et al., 2019). This implies that, on top of the spread of climate models and bias correction methods, the hydrological parameter uncertainty using GLUE is also important in climate change impact on hydrological extremes. In addition to these sources of uncertainty, the flood frequency associated uncertainty also important. Collet et al., (2017); Kay et al., (2009); Meresa and Romanowicz, (2017);Lawrence, (2020), found that the flood frequency distribution models are highly dependent on the distribution of extreme floods, the number of events, and the size and shape of the catchment.

In the last few decades, a significant effort has been given to evaluating climate change impacts on extreme hydrology, mostly focusing on low flow and high flow magnitude and trend analysis with their associated uncertainty estimation. However, there is little attention to uncertainty and impact estimation in projected flood frequency magnitude. A comprehensive uncertainty and impact estimation of climate change on flood quantile approach is developed.

1.2 Statement of the problem

Changes in major climate variables such as temperature, precipitation, and evapotranspiration are one of the most important repercussions of climate change (Mamo et al., 2019) . It is now widely acknowledged that developing countries, particularly low-income countries in tropical and sub-

tropical regions, will be disproportionately affected by the negative effects of climate change due to their lack of social, technological, and financial resources to adapt (Dale et al., 2017 and Hyeder et al., 2009).

Ethiopia is primarily reliant on rain-fed agriculture, and its geographic location and topography, along with a lack of adaptive capability, make it particularly vulnerable to climate change's negative effects (Hyeder et al., 2009). The country has experienced an increase in the frequency of flash floods in the first decade of the twenty-first century (Billi et al., 2015). During the rainy season, flash, urban, and riverine floods are common in various sections of the country, driven by significant rainfall occurrences (Mamo et al., 2019).

Climate change has impacted the Upper Awash River watershed, causing increased runoff during the wet season and decreased runoff during the dry season, resulting in increased seasonal variance in runoff and streamflow (Daba & You, 2020). The hydrological cycles of the River basin were affected by factors such as temperature, precipitation, and evapotranspiration. Therefore, evaluating the possible impact of climate change on the extreme hydrological event is essential for future development as well as for managing the current water resource development projects in adaptive way in Upper Awash River basin.

Previously, impact of climate change is conducted for Upper Awash River basin by (Daba & You, 2020 ; Getahun, 2018). In the previous research, climate models used are GCMs, CMIP3 and CMIP5 in correspondence with SRES A2, RCP4.5, and RCP8.5 scenarios using hydrological model SWAT. Now, this study aims to fill this research gap by employing climate model CMIP6 and used with HBV model to identify the impact and its associated uncertainty in flood projection. This would help to reduce numerous sources of uncertainty and their role.

1.3 Research Objectives

1.3.1 General Objective

The general objective of this study is to evaluate Peak flow Projections under the Influence of Climate Change: impact and uncertainty evaluation in the Upper Awash River Basin, Ethiopia.

1.3.2 Specific Objectives

- To compare different bias correction techniques for climate change impact assessment.
- To estimate the impact of climate change and bias correction approach on flood projections.
- To identify the source of uncertainty associated with projected flood quantiles.

1.4 Research Questions

This research has planned to answer the following questions:

- What is the impact of different bias correction techniques in climate change impact assessment?
- What is the role of HBV hydrological model parameters on future flood projections?
- What is the impact and role of climate change and bias correction, hydrological parameters on flood projections?
- What is the contribution of the main source of uncertainty associated with projected flood quantiles?

1.5 Significance of the study

Upper Awash River Basin is known commonly for its wide range of variation of climate, mainly because of climatic factors. Flood has been a common frequent phenomenon every year in one or other part of the basin. This study is expected to be helpful for the planners, decision makers and any concerned bodies to understand the consequences of flood on hydrological variables. The result of this research could be an input for those who are interested to further research in related field of study area.

1.6 Scope of the study

The purpose of this study is to investigate the impact of climate change and present the results obtained from the application of HBV Model for different climate scenarios. This study is limited to selected areas around Upper Awash catchment and the model simulations considered only future climate change scenarios assuming the land cover will remain the same at future time horizons. However, in real world the land covers change. One of the main limitations of this study is that, except temperature and rainfall all the other climate variables such as wind speed, sunshine hours, and relative humidity was assumed to be constant which is not possible in actual case.

1.7 Novelty/ Contribution of the study

The contribution of this study will be to provide information about impact of climate change on extreme hydrological events for Upper Awash River Basin by analyzing different climate scenarios and also to provide relevant information on flood magnitudes and their frequencies for design of different types of hydraulic structures and flood plain zoning, economic evaluation of flood protection projects etc.

2. LITERATURE REVIEW

2.1 Climate Change

Climate change is defined as any prolonged, systematic, and statistically significant change in long-term climate statistics such as precipitation and temperature over several decades or more (Mader, 2019). As a result, climate change can be defined as variations in long-term average precipitation or temperature, as well as variations in the frequency of extreme climate events (IPCC, 2014). The term "climate change" is frequently used to refer to climate change caused by humans (also known as global warming). Human action causes anthropogenic climate change, as opposed to changes in climate that may have occurred as a result of Earth's natural processes (Wang et al.,2016). There is a significant distinction between climate change and global warming, according to Wang et al. (2016), because global warming causes climate change.

Climate change is responsible for around 20% of the global rise in water scarcity, with countries already experiencing water shortages being the severely hit (IPCC, 2014). Water shortages and/or flooding are expected as a result of changes in rainfall patterns. Glacier melt can result in flooding and soil erosion (Dale et al., 2017). Temperature change is caused by both natural and artificial forcing's, and temperature variations cause changes in greenhouse gas concentrations (Stern and Kaufmann, 2014). Furthermore, carbon dioxide (CO2) emissions are the primary driver of global warming and are at the center of climate change mitigation discussions (Mader, 2019).

According to Dale et al. (2017), Africa is already a continent under stress from climate change and is extremely vulnerable to its effects. On seasonal and decadal time frames, several locations in Africa have climates that are among the most changeable in the world. Floods and droughts can occur in the same area within months of each other. These events can lead to famine and widespread disruption of socio-economic well-being. A considerable increase in global temperature will also reduce potential agricultural output in most tropical and subtropical regions, and some extreme events like droughts and floods will become more intense as a result of the even more unequal spatial and temporal distribution of precipitation (Haile et al. (2017).

2.1.1 Causes of Climate Changes

Climate change is the result of natural and human-caused changes to the earth's hydrologic cycles to varying degrees (Allen and Ingram, 2002). According to the IPCC (2014), human activities are responsible for roughly 95% of greenhouse gas emissions. As a result, human actions such as the burning of fossil fuels, changes in land use, such as deforestation, and the removal of forests for various purposes, all contribute to climate change (IPCC, 2014). These factors contribute to climate change by altering the levels of greenhouse gases, aerosols, and cloudiness in the Earth's atmosphere (IPCC, 2007). At a global scale, carbon dioxide (70 percent) is the primary source of greenhouse gas emissions, primarily from the burning of fossil fuels imported from industrialized countries, while other sources include methane and nitrous oxide, which are produced by deforestation and agricultural activities, particularly the use of pesticides (Haile et al. (2017).

2.1.2 Climate Change in Ethiopia

Climate change will have a huge impact, particularly in poorer countries whose economies are strongly reliant on agricultural production (Temesgen, 2000). Africa, according to the IPCC (2007), is one of the most vulnerable continents to climate change. Ethiopia's economy is heavily reliant on agriculture, as is the case in many African countries. As a result, climate change has a direct impact on the economy of the country (Simane et al., 2016). According to NMA (2001), climate variability and change in Ethiopia is mostly evident in the country's fluctuation and declining trend in precipitation, as well as an increasing trend in temperature. Ethiopia's contribution to global greenhouse gas emissions is minimal, according to IPCC (2007), but it is affected by the negative effects of climate change brought on by rich countries' carbon-intensive development pathways throughout the last century.

The annual average temperature is expected to be 26.92°C between 2070 and 2090, with average daily precipitation falling by 3.5 percent by the end of the century (Hassan, 2006).

2.1.3 Impact of climate change in Upper Awash River Basin

According to Daba et al. (2020), estimated future precipitation in the Upper Awash basin increased by 2.4 percent in 2020, but dropped in 2050 and 2080. The maximum and minimum temperatures

were both raised in all time periods. Temperature and precipitation variations can be tracked using the Area's seasonality. The authors also state that the annual streamflow of the Upper Awash basins fell in the 2050 and 2080 time periods, but increased in the 2020-time period. It suggests that streamflow and precipitation are proportionate to each other.

Climate change will have severe repercussions for water availability in the Awash River watershed, according to a study (Taye et al., 2018). The expected decrease in water availability over time indicates rising water stress in the basin and a danger of water security for the many sectors that are increasing their investments in the basin. Similarly, it is critical to recognize that factors such as population growth and land use change may play prominent roles in risking water security for the people of the basin.

2.2 Modeling Climate Change

A mathematical model called a Global Circulation Model (GCM) must be built to anticipate future climate and the impacts of anthropogenic emissions on climate. Numerical models of the atmosphere, ocean, cryosphere, and earth's surface are known as global circulation models (Ertugrul, 2019). The Regional Climate Model is driven by the GCM, which provides the beginning and lateral boundary conditions (RCM). The regional model's spatial resolution is typically tens of kilometers, but the GCM scale is an order of magnitude coarser (Taye et al., 2018). In order to estimate the impacts of anthropogenic emissions on climate, a mathematical model called a Global Circulation Model (GCM) has to be constructed of the complete climate system, which must include the atmosphere, oceans, land and cryosphere (glaciers and ice sheets). This model is a mathematical description of the earth's climate system, firstly broken down into layers (both above and below sea level) and then each grid is broken down into boxes or cells.A number of research centers around the world have developed their own versions of GCMs, but all predictions contain uncertainties. For example, because future emissions of greenhouse gases are unknown, numerous emissions scenarios have been developed; therefore, different scenarios will obviously produce different results. However, the largest uncertainty arises from the models themselves. Even if each of the different GCMs uses the same emissions scenario, they will give quite different predictions due to the different ways they represent aspects of the climate system (Meenu et al., 2013).

Physically based distributed hydrological models, which incorporate the physical laws of water movement and parameters associated with the characteristics of the catchment area and are designed to understand and approximate the general internal processes and physical mechanisms that govern the hydrologic cycle, have been found to be useful for such impact assessment studies (Meenu et al., 2013). It is possible to quantify the relevant changes in the hydrology of the basin by simulating stream flow from precipitation and temperature data collected from GCM outputs corresponding to certain climate change scenarios using an appropriate hydrological model (Chu et al., 2010).

2.2.1 Climate Change Scenarios

A scenario is a description of potential future conditions produced to in-form decision-making under uncertainty (IPCC, 2007). A climate scenario is a reasonable representation of future climate that has been constructed for explicit use in investigating the potential impacts of anthropogenic climate change. Projections of future climate variables such as precipitation and temperature as well as dependent phenomena and processes (droughts, floods etc.) are generally derived from climate models (Carter et al., 2018).

General Circulation Models (GCMs) have been developed to simulate the present climate and used to predict future climatic change because using GCM outputs considers the most valid tool, many researches have been applied in the use of these models and various emission scenarios to investigate impact of climate change (Farzaneh et al., 2012). Parameterizations of current GCMs include equations intended to reflect small scale phenomena and to approximate bulk effects of physical processes that are too complex to be represented (e.g., clouds, cumulus convection and surface albedo) (Teutschbein and Seibert, 2010). Although the functional form of parameterization is physically-based, choices of parameter values are dependent on empirical studies. In general, the input data required by GCMs typically describes Earth properties, CO2 emissions, solar energy, volcanic activity, ozone concentrations, and other boundary conditions. While GCM computations are sensitive to projected atmospheric CO2 concentrations, there is significant uncertainty regarding their future values (Carter et al., 2018). Shared Socioeconomic Pathways (SSP) were developed for the climate change research community in order to characterize future scenarios of

societal conditions in terms of the challenges they present for climate change mitigation and adaptation (Fan et al., 2020).

According to Fan et al. (2020), by the end of the 21st century, the global temperature under different scenarios is projected to increase by 1.18 °C/100 year (SSP1-2.6), 3.22 °C/100 year (SSP2-4.5), 5.50 °C/100 year (SSP3-7.0) and 7.20 °C/100 year (SSP5-8.5), with greater warming projected over the high latitudes of the northern hemisphere and weaker warming over the tropics and the southern hemisphere as shown in the table below.

Table 2.1 Shared socio-economic pathway (SSPs)

SSP	Description	Global mean temperature anomaly (^{0}C)	Global mean CO_2 concentration (ppm)
SSP1-26	2100 radiative forcing level is 2.6 W/m^2 , Medium reference scenario	1.18	230
SSP3-70	2100 radiative forcing level is 7.0 W/m2 , Medium-high reference scenario	5.5	329
SSP5-85	2100 radiative forcing level is 8.5 W/m^2 ,High reference scenario	7.2	650

2.2.2 Downscaling Methods and Tools

The procedures used to translate GCM outputs into local meteorological variables required for reliable hydrological modeling are known as "downscaling." Downscaling approaches (Chu et al., 2010) are ways for converting GCM results into local meteorological variables utilized in hydrological modeling.

Dynamic downscaling and statistical downscaling are the two types of climatic downscaling. The process of dynamical downscaling entails nesting a higher resolution Regional Climate Model (RCM) within a coarser resolution Global Climate Model (GCM) (Terink, 2009). It is used to

transfer information from GCMs to finer scales by applying a higher-resolution regional climate model (RCM) over a limited area by using GCMs as an initial and boundary conditions (Yang et al., 2010).

The statistical (empirical) downscaling approach entails the use of any of several statistical techniques that map large-scale climate GCM 'predictors' and circulation characteristics to local or regional-scale meteorological 'predictants' (Wilby et al., 2004). Essentially, statistical downscaling (SD) is a twostep process consisting of the development of statistical relationships between local climate variables and large-scale predictors, the application of such relationships to the output of large-scale output to simulate local climate characteristics in the future (Chu et al., 2010). Statistical downscaling is a realistic approach to develop a specific, local-level climate prediction. Typically, SD methods are applied to GCM projections, but may also be applied to RCM output as these results may not be representative for the local climate.

2.2.3 Methods of Bias Correction

Bias correction methods need a transformation algorithm to improve the efficiency of climate model output. The idea behind it is to recognize differences between observed and simulated historical climatic variables to parameter an algorithm used to correct simulated historical climatic data. It assumed that bias correction methods are stationary, i.e. the algorithm for correction and its parameterization is supposed to be accurate even for future conditions under the current climatic conditions (Terink., 2009). Bias correction methods facilitate the comparison of observed and simulated impacts during the historical reference period and a continuous transition into the future. Without such an adjustment of the mean behavior in the historical period, future impacts that depend on the exceedance of critical absolute thresholds of, for example, temperature (Ali et al., 2016), cannot be accurately described. Many bias correction techniques include an implicit downscaling of the simulated data to the potentially higher resolution of the observational data (Meresa et al., 2017).

2.2.4 Coupled Model Intercomparison Project (CMIP 6) Data in Africa

According to IPCC (2013) Climate models have been refined and improved over time. Many models have been transformed into Earth System models by integrating bio-geochemical cycles that are crucial to climate change. The goal of the climate model is to quantify the interactions of important climatic drivers such as the atmosphere, oceans, land surface, and ice (Flato et al.2017). Simulations aimed to test model performance under previous climate regimes are included in the Coupled Model Intercomparison Project (CMIP), which coordinates efforts to compare climate model simulations (Meresa et al., 2016). The outputs of the CMIP have been widely used in many climate change studies and in the development of the Intergovernmental Panel on Climate Change (IPCC) assessment reports (IPCC, 2013). Phase six (CMIP6) of the CMIP project is the most recent output from the World Climate Research Program (WCRP) (Cheng et al., 2016).

In comparison to the previous edition of CMIP5, the models have more value in the parameterization schemes for the climate system's major physical and biogeochemical processes (Piani et al., 2010). Recent studies that used CMIP6 found that the models performed better than those that used CMIP5 (Almazroui et al., 2020). CMIP6 models have only been used in a few studies (e.g., Almazroui et al., 2020) across Africa. Meanwhile, existing study over East Africa region mainly focused on evaluating the CMIP6 models in simulating the statistics of extreme precipitation.

Africa, the second-largest Continent on earth and with the fastest population growth, along with an economy reliant on rain-fed agriculture, is among the places most sensitive to climate variability and change (Luhunga etal.,2015). Changes in variability, extremes, and mean of temperature and rainfall make themselves felt in day-to-day life through heat stress, floods, droughts, and other impacts on both human society and natural ecosystems in Africa. However, climate change projections over Africa suffer from a lack of studies utilizing the new generation of climate models developed for the CMIP6 (Fan etal., 2020). The lowest increase in mean temperature over Africa is projected to be 1.2°C-1.4°C under SSP1-2.6 scenario for the mid- and end of the 21st century. The increase in mean temperature is projected to be 1.5°C-2.3°C under SSP2-4.5 and 1.8°C-4.4°C under SSP5-8.5 for the mid- and late 21st century. The largest increase in mean temperature (5.6°C

under SPS5-8.5) is likely in North Africa and Sahara regions which include Algeria, Morocco, Libya, Egypt, West Sahara, and Tunisia, northward of Mauritania, Mali, Chad, and Sudan. The second largest increase in mean temperature is projected over South West Africa and South East Africa regions (Birundu etal.,2017).

According to Almazroui et al., (2020), CMIP6 models (consistent with the previous generation of CMIP5 models), show a warming trend over Africa, from 1981 to the late 21st century. Furthermore, CMIP6 shows enhanced warming (1.0°C-2.5°C) over Africa compared to CMIP5 models. In other words, the latest science indicates that Africa is warming faster than was previously thought.

2.3 Hydrological Extremes and climate Change

Global warming causes changes in climate variables over time, which can have a significant impact on hydrological extremes (Meresa et al., 2017). As a result, in the context of global warming, an assessment of the potential implications of climate change on a basin's hydrology is critical (Meenu et al., 2013). Environmental changes, such as climate, have a considerable impact on extreme hydrological characteristics and accessible water resources (Meresa and Gatachew, 2018). Climate change, in particular, has a significant impact on hydro-meteorological extremes in Sub-Saharan Africa (Chaney et al., 2014; Luhunga et al., 2015). As a result, it necessitates addressing and evaluating hydrological extreme characteristics, as well as examining reciprocal reliance between flood episodes in order to identify flood-generating processes and their modification in the near and long term(Meresa, 2019).

A Research conducted by Zhang et al. (2016) , compared the potential impacts in the near future river flow using projected land use patterns and hypothetical climate scenarios. The result proves that land use changes in the near future period induce slight (non-significant) reductions in groundwater discharge and surface runoff, whereas climate change produces pronounced increases in the river flow. This shows that the joint hydrological impacts are similar to those solely induced by climate changes. This is because the global climate has been changing and it will continue changing in future due to atmospheric greenhouse gases, aerosols, and human modifications of the land surface, thus significant climate change is expected in the future (Meresa and Gatachew, 2018). However, the effects of hydrological extremes due to varying climate conditions are not fully

addressed to understand and represent the existing extreme water-related problems (Meresa, 2019). Considering variables such as flood duration, flood type, flood volume, peak flood, number of events, and flood classification will provide more understating of climate change impact on economic development and infrastructure (Liou and Mulualem, 2019).

Floods are one of the most common quantiles in the world which cause loss of lives, livelihood and property damage. The occurrences of floods in mountainous regions are now more common and more frequent due to global warming (Ali et al., 2016). Flood risk increases as people seek the benefits of living near water and it is one of the most significant environmental and societal challenges (Mamo et al., 2019). Even though there is no evidence of a direct relationship between the increased frequency of extreme events and climate change, the observed positive trend indicates an increased probability of urban flooding and flash floods. Additionally, changes in land use, such as urbanization, a decrease of natural retention and poor water management may strongly influence the number of extreme (flood and drought) events (Meresa et al., 2016).

Ethiopia had extensive experiences in both flash and riverine flood events, the history of flood events and their spatial extents were evaluated since 1960s to present (Mamo et al., 2019). According to Billi et al. (2015), flash floods are posing constraints to the economic growth and the development process of the country and in order to mitigate such quantile, it is crucial to understand the relative roles of two main factors such as rainfall intensity and land use change.

2.4 Hydrological Modelling

Hydrological modeling is a widely used technique for predicting the hydrological response of a basin to precipitation. It enables researchers to forecast the hydrologic response to various watershed management strategies and gain a better knowledge of their effects (Kalita et al., 2019; Putty and Prasad, 2000). According to Mamo et al. (2019) Hydrological modeling is a powerful technique of hydrological systems investigation for both the research hydrologist and practicing water resources engineers involved in the planning and development of an integrated approach for the management of water resources.

On the basis of process description, the hydrological models can be classified into three main categories: lumped, semi-distributed and distributed models (Billi etal., 2005). The parameters in

lumped models frequently do not represent physical aspects of hydrologic processes and they do not vary spatially within the basin, basin response is examined only at the outlet (Simane et al., 2016). Semi-distributed (simplified distributed) model's parameters are partially allowed to vary in space by dividing the basin into a number of smaller sub basins. Models based on kinematic wave theory (KW models, such as HEC-HMS and HBV) and probability distributed models (PDM models, such as TOPMODEL) are the two primary forms of semi-distributed models (Beven, 2007). Distributed models' parameters can fully fluctuate in space at a resolution that is normally specified by the user. For parameterization in each grid cell, distributed models typically require vast volumes of (sometimes unavailable) data (Aven,2019).

2.4.1 Hydrological Model Selection Criteria

There are currently a number of hydrological models available that simulate the hydrological process at various spatial and temporal scales. Although there are no hard and fast rules for selecting models, some simple recommendations can be mentioned (Chaney etal., 2014). However, one of the most important things that should be considered during hydrological model selection is availability of input data to model the watershed (Cheng et al. 2017). Subsequently the simplest method that can provide the answer to the questions has to be chosen. Among the various project-depended selection criteria, there are four common, fundamental ones that must be always answered:

1. Required model outputs important to the project and therefore to be estimated by the model (Does the model predict the variables required by the project such as peak flow, event volume and hydrograph, long-term sequence of flows …?),

2. Hydrologic processes that need to be modeled to estimate the desired outputs adequately (Is the model capable of simulating regulated reservoir operation, snow accumulation and melt, single-event or continuous processes?),

3. Availability of input data (Can all the inputs required by the model be provided within the time and cost constraints of the project?),

4. Price (Does the investment appear to be worthwhile for the objectives of the project?).

2.4.2 The HBV model

Swedish Meteorological and Hydrological Institute developed the HBV model, which is a semi-distributed conceptual rainfall runoff model (Bergstrom, 1995; Lindstrom et al., 1997). It has been widely utilized in hydrological simulations and has been employed in a variety of studies for design floods, flood forecasting, and climate change research (Driessen et al. 2010; Al-Safi & Sarukkalige 2017). The model has 12 parameters that need to be parameterized for calibration. Monte-Carlo (MC) simulations can be performed using random numbers from a uniform distribution within the set ranges for each parameter as shown in the Table 2.2. The model is subdivided into three routines; snow and glacier routine, soil moisture routine and runoff generation routine.

The snow and glacier routine use a temperature-index method to calculate snow and ice melt. Input data are daily air temperature and precipitation. Changes in precipitation and Inputs into the model are precipitation, air temperature, runoff, PET and catchment description. Precipitation and temperature data from meteorological stations need to be corrected for measurement errors. Runoff is taken from the selected gauging stations (Driessen et al., 2010). Catchments can be separated into different elevation/vegetation zones and sub catchments. The model uses sub basins as primary hydrological units and within these an area-elevation distribution and a classification of land use (forest, open and lakes) can be made. The main output is discharge, although other output variables related to water balance components (precipitation, evapotranspiration, soil moisture, water storage) are available from the model (IHMS, 1999).

2.4.3 Why the model was selected

HBV was chosen because of its flexibility, computational efficiency, proven effectiveness under a wide range of climatic and physiographic conditions [e.g., Zhang and Lindstrom, 1996; TeLinde et al., 2008; Steele-Dunne et al., 2008; Breuer et al., 2009; Driessen et al., 2010; Deelstra et al., 2010; Plesca et al., 2012; Beck et al., 2013a; Bouffard, 2014; Demirel et al., 2015; Vetter et al., 2015],.The model is capable in conducting hydrological analysis related to the water balance is well known and it has been used in more than 30 countries (Bergstrom, 1992). According to Das et al. (2008), physical based parameters are the important strengths of the HBV model and is simple to link them to physical attributes; HBV model has an excessive number of free parameters as compared with

other models. HBV demands simple data; it is user-friendliness; it's operation is easy ; it has high level of performance (Lindström et al. 1997).

In the study done by Unduche et al. (2018) evaluation of the four models for flood forecasting which are WATFLOOD, HBV, HEC-HMS and The Hydrologic Simulation Program-Fortran (HSPF); have shown that HBV model perform better in forecasting the runoff of the next year and that it performs better in simulating high flows (Kobold et al. 2006).

2.5 Researchable Issues in using HBV Model

Birundu et al.(2017) applied a semi-distributed HBV Light Model to stimulate the rainfall runoff in the Mara River Basin, Kenya. The research shows that the model was not able to stimulate well the flow peaks in the catchment as it over estimated flow peaks despite being able to properly stimulate the recession flow hydrograph; this could be attributed to the fact that missing values in the data set were filled by interpolation which may have increases errors in the model.

According to Badilla (2008), Flood Modeling in the Pasing-Marikina River Basin, the HBV model has uncertainty that comes from a variety of sources, including input data used to represent the model's condition in space and time, recorded data used to evaluate the simulation's result, and uncertainties caused by the calibration process and model simplification. In most cases, the HBV model overestimates low flow (Unduche et al., 2018). Because of uncertainties in input data, differences between basin physics and model structure, model calibration, and changes in catchment characteristics over time, the simulated hydrograph can differ from the observed hydrograph (Roth et al., 2018).

Lawrence et al. (2009) conducted a study on calibrating HBV hydrological models using PEST parameter estimation. In this study, HBV hydrological models were calibrated for 117 unregulated catchments using 1 x 1 km grid-based precipitation and temperature input data, and five best fit models were calibrated for each catchment using PEST parameter estimation routines based on observed streamflow. This study shows some weakness of the HBV model, the first weakness in the model results which applies to all catchments is that the simulations tend to underestimate flood peaks, the second weakness associated with input data, some of the smaller catchments have poorer

model fits, possibly due to a mismatch between the HBV model time step and the runoff response in these catchments.

2.6 Related Studies in Ethiopia

Meresa and Gatachew (2016) evaluate the predicted influence of climate change on hydrological extremes in selected catchments in the upper Blue Nile river basin, as well as the implications for water resource management and planning. For this, they employed seven future projection runs of the CORDEX Regional Climate Model based on the CMIP 5 RCP 2.6, RCP 4.5, and RCP 8.5 scenarios. Using distribution-based quantile mapping, the run results for daily rainfall, minimum and maximum temperatures were bias adjusted against observed data. They find that climate change may have a positive impact on the distribution of hydrological extremes in the research area in most portions of the northern, western, and northeastern parts of the river basin.

Despite the fact that both climatic variables are expected to rise in the future, the rise in monthly average precipitation appears to be overshadowed by the rise in monthly average temperature. As a result, total annual inflow volume into Lake Ziway might drop by as much as 19.47 percent in A2a scenarios and 27.43 percent in B2a scenarios. The decreasing trend of the average annual inflow volume is mainly associated with the decrease in the *Kiremt* inflow volume by between 11.8 and 28.4% for the A2a scenario and between 16.5 and 27.8% for the B2a scenario (Zeray, 2006). Also Tarekegn and Tadege, (2006), studied the effects of climate change on the water resources of the Lake Tana-sub basin. The finding demonstrates that if the temperature is raised by 20 degrees Celsius while rainfall remains constant, the mean annual flow will decrease by 11.3 percent.

3. DESCRIPTION OF THE STUDY AREA

3.1 Location

The Awash River Basin is one of Ethiopia's 12 river basins. It drains the country's center and eastern highlands. Its catchment area is approximately 110,00 km2 (Edossa et al., 2010). The river begins at an elevation of 3000 meters above sea level (m.a.s.l) in Ginchi, west of Addis Ababa, and travels all the way along the rift valley, ending at an elevation of 250 meters above sea level (m.a.s.l) in Lake Abe on the Ethiopian-Djibouti border at an altitude of 250 meters above sea level (m.a.s.l) with a total length of about 1200 kilometers (Bekele et al., 2019).

The basin is located at latitudes of $7^0$53'N and 12^0N, and longitudes of $37^0$57'E and $43^0$25'E and constitutes the central and northern part of Rift valley and is bounded to the west, southwest, and south by Blue Nile, the Rift Valley lakes, and Wabi Shebele basins, respectively The high, middle, and lower basins of the Awash River basin are separated into three sections. Based on climatological, physical, socioeconomic, agricultural, and water resource characteristics, the Awash River basin is classified into three parts: upper, middle, and lower basins (Edossa et al., 2010). According to the Awash Basin Authority, the total annual water demand by the four sectors is estimated to be 3.4 BCM (Billion Cubic Meter), 0.3 BCM, 0.12 BCM and 0.28 BCM for irrigation, domestic, livestock and industrial uses, respectively. The area considered for this research only covers upper part of the Awash basin which is located in central Ethiopia at the western margin of Rift valley and situated between 8° 23' 25" to 9° 18' 42" N latitudes and 37° 59' 9" to 39° 04' 12" E longitudes (Figure 3.1). The upper part of the basin upon delineation using the 30 m resolution digital elevation model (DEM) in the Hombole River gauging station covers the area of 7,628 km^2.

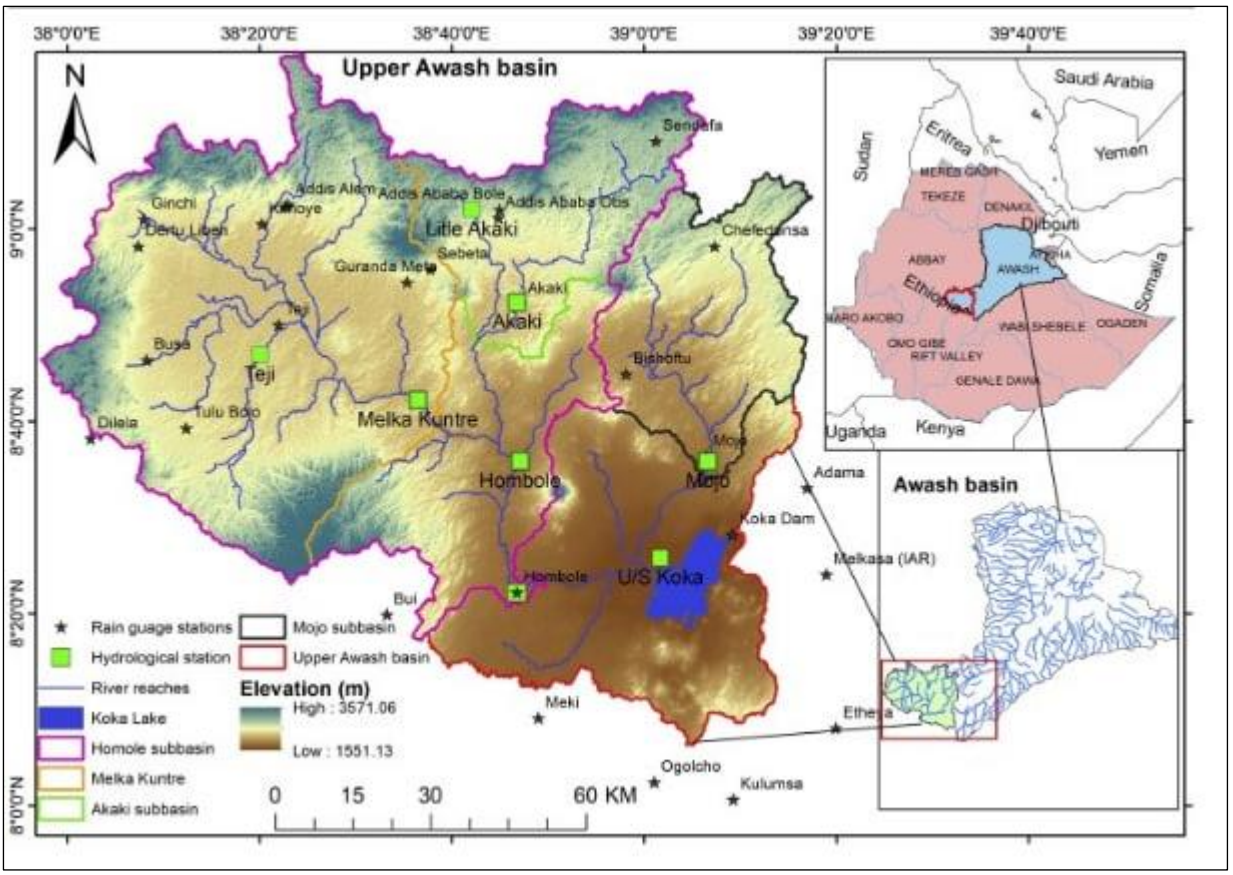

Figure 3.1 Location map of the study area

3.2 Climatic condition

The Inter-Tropical Convergence Zone (ITCZ) has an impact on the climate of the Awash River basin. The annual migration of the ITCZ determines the seasonal rainfall distribution within the basin. The catchment receives the most rain from June to September, accounting for 70 to 75 percent of the annual precipitation. From February until May, the second rainy season takes place. The relative humidity in the Upper Awash varies from 49 percent to 85 percent. The relative humidity approaches 80% during the rainy season (June, July, and August). In comparison to the wet season, however, the relative humidity of the dry season is low. In November and December, wind speed reaches its highest point (4 m/s) and its lowest point (below 1 m/s) during the rainy season (June to August).

The average length of sunshine hours become above 8 hours per day in October to December. However, it substantially decreases in the rainy periods (below 4 hours per day). The pan evaporation is about 180 mm during the dry season of November and 75mm/month in the wet season (June, July and August) at Addis Ababa observatory.

3.3 Land use and soil type

The land use condition in the upper Awash catchments includes mainly of cultivated agricultural land, grassland, and forestland, rural and urban settlements. It is estimated that 67% is intensively cultivated, 25.5% is moderately cultivated, 4.5% is bush land or shrub land or wooded grassland, and 3% is urban area and alpine vegetation. Strictly speaking, even the land use within the upper Awash is diverse. In the upper most part where there is high rainfall, land use is complete in May with barley and teff. On the lower most part, however, rainfall is too unreliable and the sparse dry acacia scrub gives way to wide stretches of bare ground with clumps of coarse grass and occasional thickets of acacia. In UAB, vertisols are the most common soil type (Figure 3.2). Cambisols are the next most common type of soil in the basin, followed by Luvisols and Nitisols, which are found on the leaves and former channels of the Awash River and its tributaries to a lesser extent.

The Vertisols in the basin are black clay soils characterized by the clay mineral montmorillonite. In the dry season, this mineral swell when moist and shrinks when dry, generating surface fractures. The cracks are well developed into inundated areas and back swamps of the plains where they can be 10 cm wide and 70 cm deep .Land use and soil type have a direct impact on the amount, extent and speed of the flood and hence can influence the magnitude of flooding.

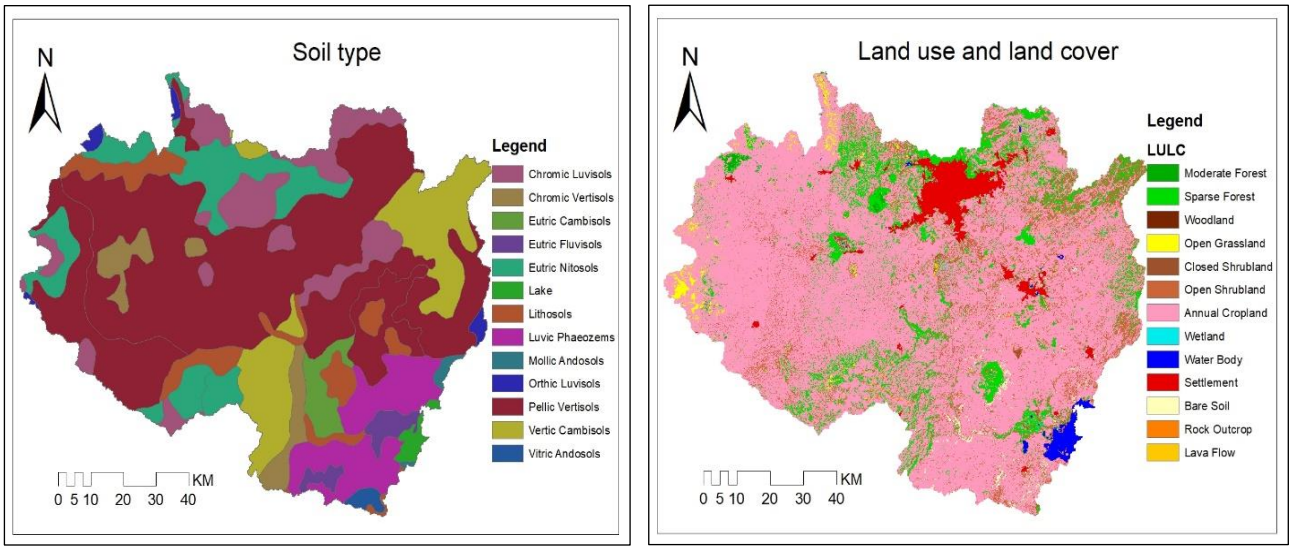

Figure 3.2 Soil type and LULC of UAB

3.4 Datasets

For this study, meteorological and hydrological data were used. Meteorological data (daily rainfall, and temperature) from National Meteorological Service Agency (NMSA), hydrological data (daily historical streamflow) and soil data have been collected from Ministry of Water, Irrigation and

Electricity (MOWIE), and land use land cover data from Ethiopian Mapping Agency (EMA) was collected.

Table 3.1 illustrates the spatial and temporal resolution of each data, the sources in which the data obtained and the importance of data in the process of the study.

Table 3.1 Data sets used in the study

Data sets	Spatial Resolution	Temporal Resolution	Source	Description
Observed precipitation data	Point data	Daily	National Meteorological Service Agency (NMSA)	Used as an input for hydrological model HBV
Temperature (max &min)	Point data	Daily	National Meteorological Service Agency (NMSA)	Used to estimate potential evapotranspiration (PET), which is latter used as an input for HBV to simulated flood flow
Observed stream flow data	Point data	Daily	Ministry of Water Irrigation and Electricity (MoWIE)	Used in calibration, validation and performance evaluation of HBV model
Digital Elevation Model (DEM)	30 m x 30 m		USGS earth explorer	Main input for study area delineation

3.4.1 Historical Hydro-Meteorological Data

The historical daily precipitation and temperature for fifteen stations and streamflow data records of five stations were taken from National Meteorological Agency (NMA) and Ministry of Water and Energy from 1981-2017 and 1981-2010 periods respectively. The selected stations are located inside and near Upper Awash River basin (Figure 3.3). The watershed for the study was delineated by using ArcGIS 10.4 and DEM of 30 by 30 downloaded from SRTM was used to delineate the Study area (Figure 3.3).

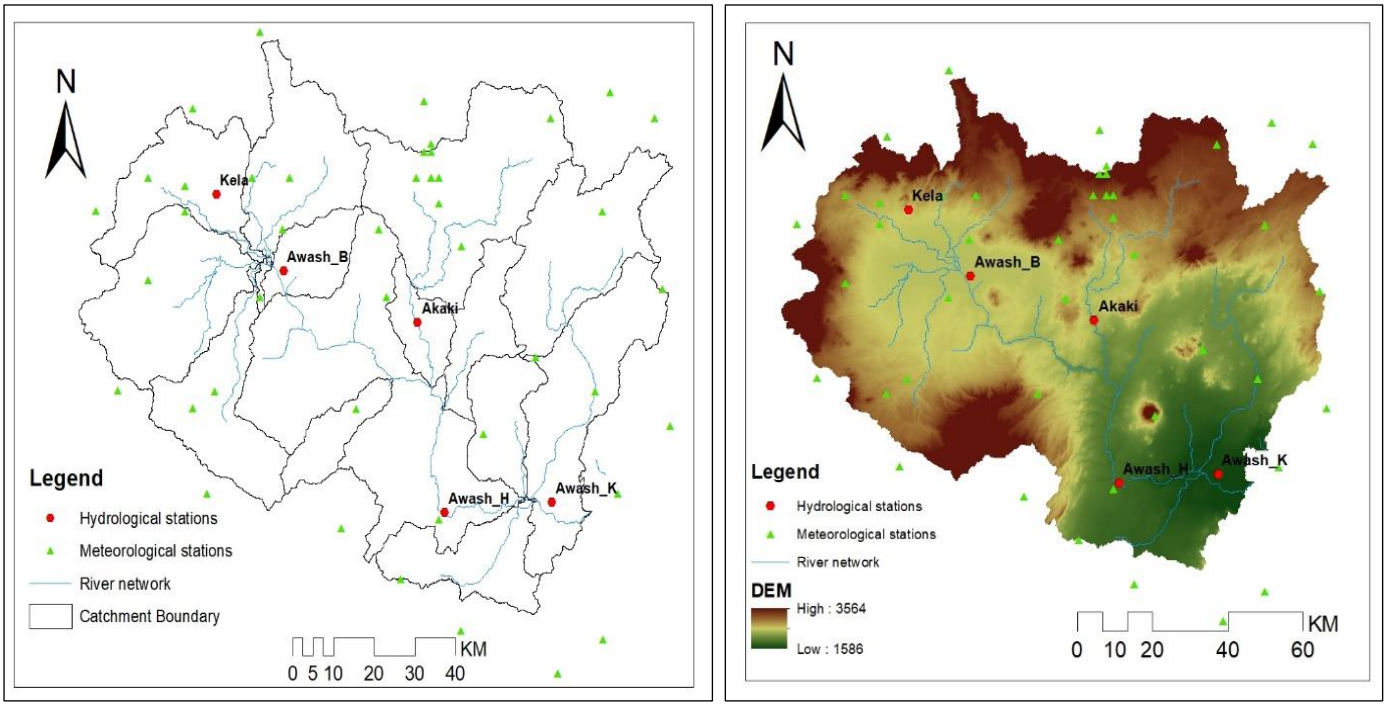

Figure 3.3 Location of hydro-meteorological Stations and Digital Elevation model of UARB

3.4.2 Future data

In this study, 12 climate models and three CMIP6 scenarios (SSP1, SSP3, SSP5) were used to evaluate the projected flood quantile's impact and uncertainty in the selected Upper Awash catchments (see Table 4.3 for climate model name and model details). The climate models listed in Table 4.3 are all global models with 50-250 km resolutions. This GCMs (CMIP6) can capture the variability and seasonality of precipitation and temperature better than those with high resolution (Almazroui, 2020).

3.5 Data availability

In this study, 15 stations that having meteorological variables (rainfall, maximum & minimum temperature) was obtained from NMSA.

Table 3.2 Meteorological stations used in the study

No	Station Name	Lat (^{0}N)	Lon (^{0}E)	Altitude (m a.s.l)	Period of record	RF	Tmax	Tmin	Class	Total missed data (%)
1	A.A obs.	9.02	38.45	2354	1981-2017	√	√	√	1	1.18
2	Bantuliben	8.37	38.22	2160	1981-2017	√	X	X	4	26.04
3	Boneya	9.48	38.39	2310	1981-2017	√	X	X	4	8.14
4	Busa	8.5	38.07	2200	1981-2017	√	X	X	4	19.61

5	D/Zeit	8.73	38.95	1900	1981-2017	√	√	√	1	14.67
6	Ejersalele	8.15	38.41	1900	1981-2017	√	X	X	4	2.43
7	Enselale	8.56	38.32	2200	1981-2017	√	X	X	4	16.21
8	Ginchi	9.03	38.12	2290	1981-2017	√	X	X	1	12.15
9	Hombole	8.22	38.46	1800	1981-2017	√	X	X	1	32.16
10	Jeldu	9.2	38.32	2300	1981-2017	√	√	√	4	7.67
11	Sebeta	8.59	38.38	2240	1981-2017	√	X	X	4	11.06
12	Sendafa	9.15	39.02	2550	1981-2017	√	X	X	4	17.18
13	Tulu Bolo	8.67	38.22	2100	1981-2017	√	√	√	1	8.45
14	Wolisogiyo	8.31	37.58	1960	1981-2017	√	√	√	1	4.56
15	Zuquala	8.55	38.83	3050	1981-2017	√	X	X	4	22.06

Five sub-catchments were selected for climate change impact assessment. They are located in different geographical and hydro-climatic conditions: Awash_K (at U/S of Koka), Akaki (at Aba S), Kela (at Welen), Awash_B (at Bello), and Awash_H (at Melka H) catchments are most representative for flood quantile estimation under varying climate conditions. These selected catchments' drainage area ranges from 67.5 km^2 (at Welen) to 7093.9 km^2 (U/S of Koka) and catchments elevation varies from 1602m (U/S of koka) to 2300m (at Melka H).

Table 3.3 Statistical description of the five selected gauged stations

Code	S1	S2	S3	S4	S5
River/Lake	Awash_K	Akaki	Kela	Awash_B	Awash_H
Guage at site at/Nr	U/Sof Koka	Aba S	Welen	Bello	Melka H
Latitude [degree]	8.4	8.75	9	8.85	8.38
Longitude [degree]	39.02	38.72	38.27	38.42	38.78
Elevation [m]	1602	1994	2129	2060	2300

4. METHODS

The methods that were used include desk study of the previous study on different basins, data collection from institutions such as Ministry of water resource, National meteorological agency and etc. After collecting the necessary data for the research delineation of the study areas, determination of basin characteristics, and analysis of rainfall and stream flow data was made. Then, the hydrological model is calibrated and validated for the baseline period and the assessment of impacts of climate change on the study area is carried out by incorporating HBV model and the future rainfall and temperature data that was obtained from Coupled Model Inter comparison Project Phase 6 (CMIP6).

4.1 Data Processing and Analysis

4.1.1 Filling Missing data

All the gauging stations may not have accurately filled and even if the data are recorded, they may have some defect since there is a possibility that they are influenced of natural and man-made factors. Other stations may have short record length. In those cases, filling missed values and checking the quality of the recorded values will be done. The arithmetic-mean and normal ratio method was selected to fill in missed rainfall and temperature data in this study. Missing rainfall data was filled by the arithmetic mean method (when the normal annual rainfall (NARF) of the surrounding station failed to be within 10% of NARF of missed station) and normal ratio method (when NARF of all surrounding stations are within 10% of NARF of missed station). Missed value for temperature was filled using the arithmetic mean method. A total of 15 stations for rainfall and 5 stations for temperature (Tmax & Tmin) were used to fill in missed values. Equations used to fill missing meteorological data presented in appendix A1 and defined by equations A1 and A2.

4.1.2 Homogeneity and consistency test

Finishing filling missed rainfall data is followed by testing and checking homogeneity and consistency of rainfall data. The homogeneity of rainfall gauging stations was tested by computing and making non-dimensional the rainfall data (pi) by dividing monthly time series data by the average rainfall amount of the corresponding month. Figure 4.1 Illustrates the homogeneity of all the 15 stations used in the study, in which almost all stations show a homogenous pattern of rainfall and the maximum rainfall consistently occurs in months from June to September. The rainfall for all stations was unimodal in nature.

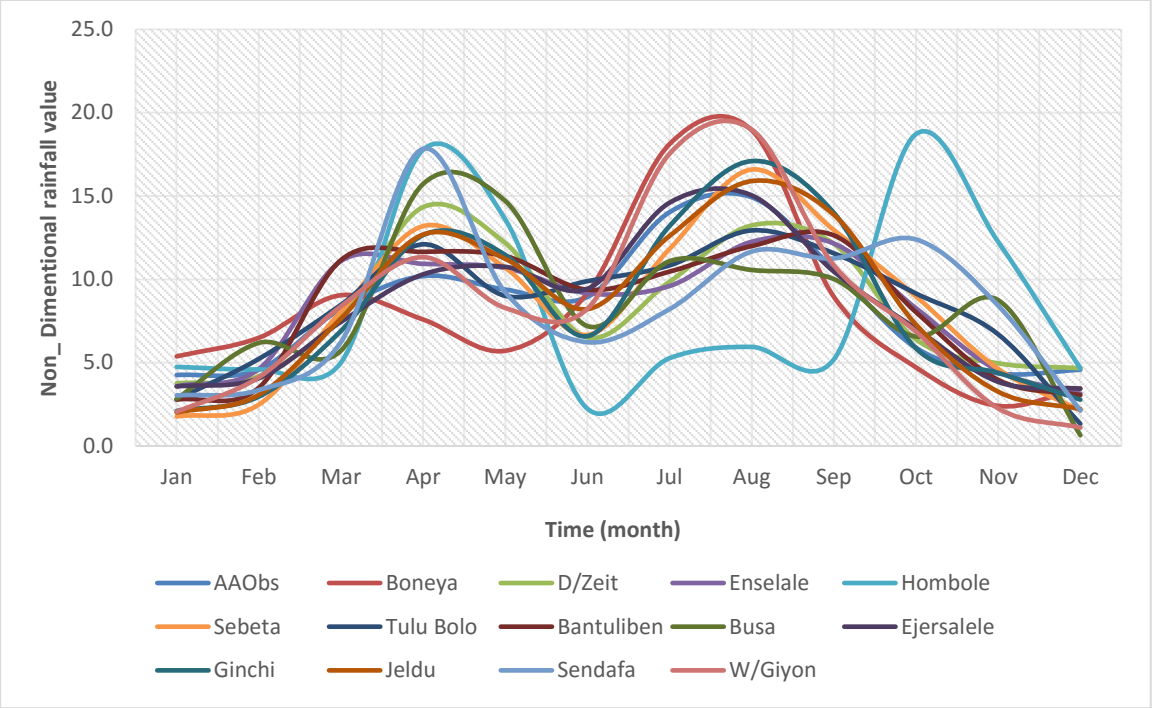

Figure 4.1 Homogeneity test of rainfall stations of UAB

Checking the consistency of individual stations, the data qualities with regard to possible temporal variations or errors been investigated by a double mass curve (DMC). DMC plotted using the cumulative annual rainfall of stations in question against the concurrent cumulative annual rainfall for a group of surrounding stations for data record years from 1986 to 2017. For the stations (sebeta, Busa, enselale and Hombole) showing inconsistency in record slope correction was applied to make the station consistent (equation A3 in appendix A used for slope correction). Figure 4.2 shows that most of the rainfall stations show consistency in the record while non-significant inflection in slope for station Boneya and Zequala was reported, and necessary adjustment was applied by using a slope correction method.

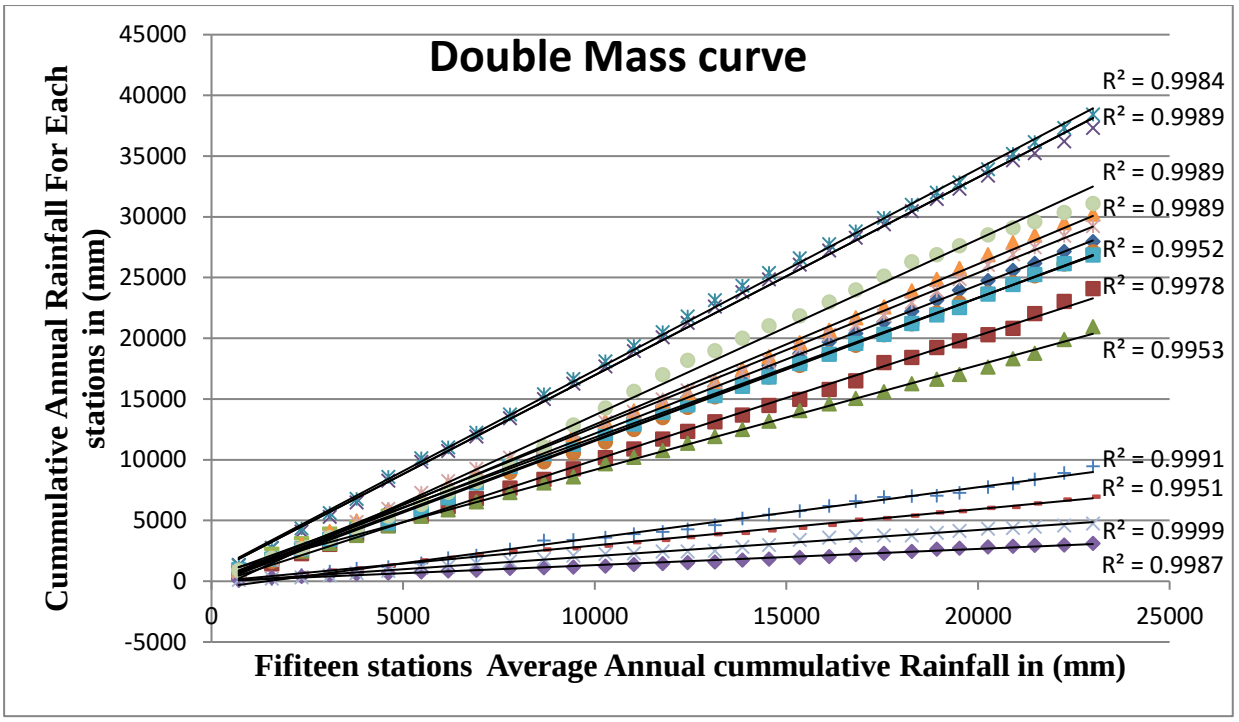

Figure 4.2 Double mass curve of rainfall data

4.1.3 Potential evapotranspiration (PET)

Potential evapotranspiration (PET) is one of the important input parameters for rainfall-runoff modeling. The estimation of station PET was computed by the Hargreaves method. This method was selected hence it demands less amount of data and could attain high accuracy (Samani, 2000). Using this input data station estimate of PET is calculated and then sub-catchment PET computed using point PET. Five meteorological stations found inside and outside the study area were used to estimate station PET in this study.

4.2 Bias correction techniques

Global and regional climate models are essential for enlightening our understanding of annual, seasonal, and daily precipitation and air temperature characteristics. These climate models are constructed based on atmospheric-land-ocean interaction, which is a complex and dynamic mathematical representation of the physical process. This results in all climate models exhibit biases in their outputs (Giorgi & Gao, 2018;Krinner & Flanner, 2018), making it challenging to develop accurate and reliable climate information. Some studies have confirmed that the prerequisite to post-processing in the climate models output before i

ts routine in hydrological extremes projections (Ehret et al., 2012; Teng et al., 2012; Meresa and Romanowicz, 2017;Osuch et al., 2017). However, minimizing the bias in climate model output

is still a big challenge. There is a problem in finding/developing a robust climate bias correction technique that reduces the biases between the observed and simulated climate data in the historical period. In the past and recent times, several studies have shown mixed results in methods and evaluation of bias correction methods in precipitation (including intensity and wet days) and temperature data. For instance, Teutschbein & Seibert, 2013;Yang et al., 2010 showed the distribution mapping based on theoretical distributions outperforms compared to other bias correction methods in their result.

Similarly, (Berg et al., 2012 &Chen et al., 2013), documented that theoretical distribution mapping performs similar to, or only marginally better than, empirical quantile mapping or other statistical methods. Contrary, Gudmundsson et al., 2012;Gutjahr & Heinemann, 2013;Lafon et al., 2013 concluded that empirical quantile mapping demonstrates higher skill than theoretical distribution mapping in systematically correcting RCM precipitation. In this study, three climate bias techniques used to correct the raw climate output and examine the contribution of bias correction methods to the flood quantile magnitude and frequency.

4.2.1 Statistical quantile factor change (SQF)

This study proposed a new bias correction technique to compare with the commonly used methods (DQM and EQM). The statistical quantile factor changes technique (SQM) of bias correction is a direct and straightforward precipitation correction, considered a simple error transfer from the historical to a future period. This involves correcting the future daily precipitation ($P_{fut,corr}$) by multiplying the average reciprocal ratio of observed precipitation (P_{obs}) and reference precipitation simulation ($P_{ref,raw}$) to the prediction of raw climate model precipitation ($P_{fur,raw}$). Whereas, for correcting future air temperature ($T_{fut,corr}$), it is by adding the difference in observed air temperature (T_{obs}) and simulated by climate model at reference period ($T_{ref,raw}$) to raw climate output ($T_{fur,raw}$).

$$P_{fut,corr} = \frac{P_{fur,raw}}{2} * \left[\frac{P_{obs}}{P_{ref,raw}} + \frac{P_{ref,raw}}{P_{obs}}\right] \quad (1)$$

$$T_{fut,corr} = T_{fur,raw} + \min(\left(T_{obs} - T_{ref,raw}\right), \pm 2.2) \quad (2)$$

4.2.2 Distribution Quantile Mapping (DQM)

Distribution quantile mapping is a parameter bias correction technique that depends on the type of distribution fitted to observed and simulated climate data (Piani et al., 2010). This

distribution-based approach can be Single or Double Distribution Quantile Mapping (S/DQM) or other distributions. The excess number of dry days, drizzles, and wet days were considered and properly corrected in this method. For every N year, remove the zero precipitation, and the single Gamma distribution is fitted to the upper 75 % of daily precipitation. In contrast, the double Gamma distribution fitted to both upper and lower parts of 75 % of the daily precipitation.

$$P_{corr} = F_{dg}^{-1}(F_{dg}(P_{raw}(t), \alpha_{raw}, \beta_{raw}), \alpha_{Obs}, \beta_{Obs}) \quad (3)$$

$$T_{corr} = F_{dn}^{-1}(F_{dn}(T_{raw}(t), \alpha_{raw}, \beta_{raw}), \alpha_{Obs}, \beta_{Obs}) \quad (4)$$

Where P_{corr} and T_{corr} stand the bias-corrected daily precipitation and temperature, respectively. Likewise, and represent raw climate output, daily precipitation, and air temperature.

The raw climate output inverse cumulative density is symbolized by F_{dg}^{-1}, and $P_{raw,}$ T_{raw} for precipitation and temperature, respectively. The dn and dg subscripts stand for the normal (for temperature) and Gamma (for precipitation) distributions. The Gamma (for precipitation) distributions has two parameters, shape and scale parameters are symbolized by α and β and the normal (for temperature) distribution standard deviation and mean by σ and μ, respectively.

4.2.3 Empirical quantile mapping (EQM)

Unlike the distribution mapping approach, the empirical quantile mapping is based on a paired-wise comparison between empirical cumulative density function (ecdf) of observed and simulated precipitation at reference period. This is purely empirical and direct matching of the histogram of the observed to the future period. The future precipitation and temperature are corrected using the inverse of ecdf ($ecdf^{-1}$) and fitted ecdf .

$$P_{hst,m,d}^{cor} = (ecdf_{obs,m}^{-1}(ecdf_{hst,m}(P_{hst,m,d}))) \quad (5)$$

$$T_{hst,m,d}^{cor} = (ecdf_{obs,m}^{-1}(ecdf_{hst,m}(T_{hst,m,d}))) \quad (6)$$

4.3 Bias correction performance evaluation

The performance of the selected statistical bias correction technique was evaluated using four statistical measures: Correlation coefficient (RR), Mean Absolute Error (MAE), Root Mean Square Error (RMSE), Percent of Bias (PBIAS), and Maximum precipitation weighting root means square error (MPWRMSE). These statistical measures were applied to daily rainfall and temperature time series of climate model output. The time series-based evaluation was performed by comparing the capacity of each approach to generate precipitation and temperature.

$$RR = \frac{\sum(P_S - \bar{P_S}) * (P_C - \bar{P_C})}{\sqrt{\sum(P_S - \bar{P_S})^2 * \sum(P_C - \bar{P_C})^2}} \quad (7)$$

$$MAE = \frac{\sum_{i=1}^{n} |P_S - P_C|}{N} \quad (8)$$

$$PBIAS = \frac{\sum_{i=1}^{n} |P_S - P_C|}{\sum_{i=1}^{n} P_S} \quad (9)$$

$$PWRMSE = \left[\frac{\sum_{i=1}^{n} |P_S - P_C|^2}{N}\right]^{0.5} \quad (10)$$

Where Ps is observed precipitation at given station, Pc is corrected precipitation, N number of observations. We also used similar performance criteria for daily air temperature bias correction methods.

4.4 Coupled Model Intercomparison Project phase 6 (CMIP6)

CMIP6 is a new climate dataset project (https://pcmdi.llnl.gov/CMIP6/) which was released by a collaborative effort of different climate research institutes to advance climate change knowledge and applicability. The daily time scale of precipitation and air temperature time series from the CMIP6 simulation datasets (https://esgf-node.llnl.gov/search/cmip6/) were used for impact estimation. The climate model's output covers 1971-2100 periods and provides global scale spatial resolution, ranging from 50-250km. The three Shared Socioeconomic Pathways (SSP) scenarios used from CMIP6 archive are SSP1-26 (lower level), SSP3-70 (middle level), and SSP5-85 (high level).

In this study, 12 climate models and three CMIP6 scenarios (SSP1, SSP3, SSP5) were used to evaluate the projected flood quantile's impact and uncertainty in the selected Upper Awash catchments. Each grid data of daily temperature and precipitation time series are extracted from the gridded data overlaying the catchment centroid point. The climate models listed in Table 4.3 are all global models with 50-250 km resolutions. This GCMs (CMIP6) can capture the variability and seasonality of precipitation and temperature better than those with high resolution (Almazroui, 2020).

The new climate data set (CMIP6) is used for the first time for climate change impact study in Ethiopia. Many climate and environmental research institutes contribute to Coupled Model Intercomparison Project phase 6 (CMIP6) dataset development (Wyser et al., 2019). CMIP6 dataset is more sensitive to extreme climate variables than CIMP5, which implies more significant warming and intense projections. The unique characters of CIMP6 (differ from the previous climate datasets (SRES, CORDEX)) lead to having an impact on hydrological

components. So far CIMP6 is not tested and verified for extreme hydrological projections. Therefore, it is novel and essential to use and evaluate the CIMP6 climate dataset to projections hydrological extremes in selected upper awash catchments.

Table 4.1 List of climate models used in this study

Institute	Parent source Id
Commonwealth Scientific and Industrial Research Organization, Australia	ACCESS-CM2
Beijing Climate Center, China	BCC-CSM2-MR
National Center for Atmospheric Research, USA	CESM2
European: EC-EARTH consortium	EC-Earth
Global Fluid Dynamics Laboratory, USA	GFDL
Met Office Hadley Centre, UK	HadGEM3-GC31-LL
JAMSTEC, AORI, NIES , and R-CCS, Japan	MIROC6
Max Planck Institute for Meteorology, Germany	MPI-ESM1-2-HR
Meteorological Research Institute, Japan	MRI-ESM2-0
Nanjing University of Information Science and Technology, China	NESM3
NorESM Climate modeling Consortium, Norway	NorESM2-LM
Met Office Hadley Centre, UK	UKESM1-0-LL

4.5 Hydrological modelling

Many hydrological models were developed to understand hydrological processes in local and global spatial scales. There are vast ranges of hydrological model types; most of the hydrological models have a considered physical mechanism and empirical equations to describe the catchment processes. The hydrological parameter set is one type of uncertainty source in extreme hydrological modeling.

The Hydrologiska Byråns Vattenbalansavdelning (HBV) ((Bergström, 1981) is widely applied in different hydro-climate conditions of the world (Meresa and Gatachew, 2018; Meresa et al., 2017; He et al., 2018). HBV is mainly designed to simulate daily streamflow using daily precipitation, daily air temperature, and evapotranspiration estimated using Hargressive method Hamon, (1964); are the primary climate variable that are used as inputs to the model. It is a daily lumped conceptual hydrological model and applied in many parts of the world (Meresa et al., 2017;Meresa & Gatachew, 2018). In this study, HBV was used with nine parameters (Table 4.4 and Figure 5). This model structure has three consecutive stores: one related to the surface, the second associated with the saturated soil layer, and the other to the unsaturated routing store. The

detailed information about the model is described in Bergström, 1981. The upper and lower limits of the hydrological model are listed in Table 4.4 and Figure 5. The detail of these hydrological models, including their physical meaning and description of each model parameter, are explained Bergström, 1981.

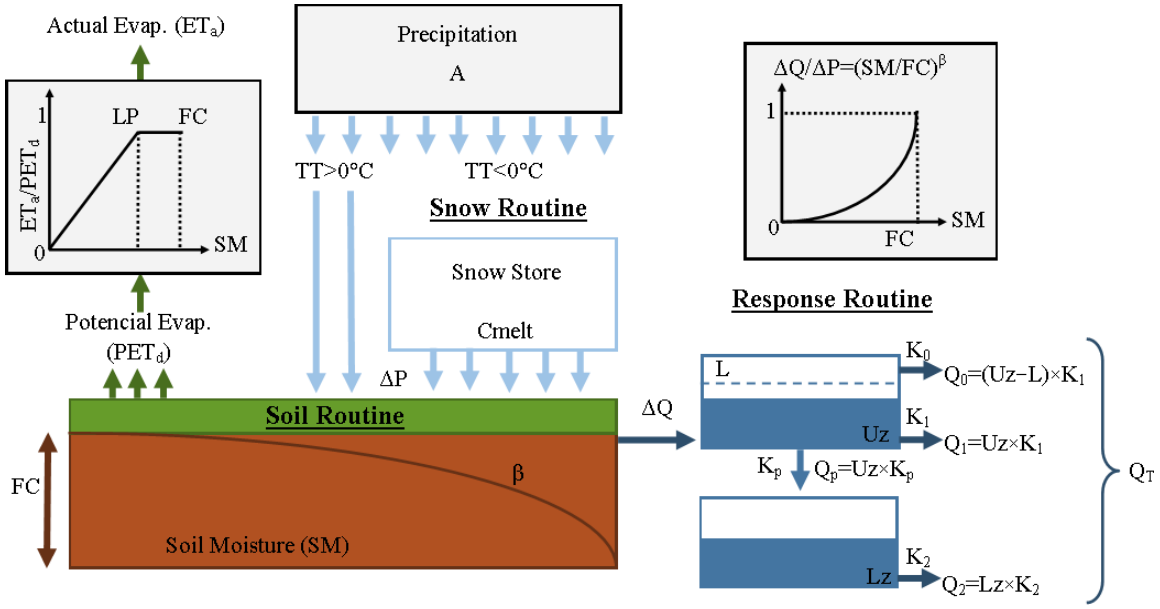

Figure 4.3. Hydrologiska Byråns Vattenbalansavdelning (HBV) hydrological model structure (Bergström, 1981)

The water supply (rainfall) flows through the soil component, where the amount of water contributing to the upper reservoir's recharge is determined by antecedent soil moisture, field capacity (FC), and a shape parameter (BETA). Through evapotranspiration, a portion of the soil moisture is released into the atmosphere. The latter is calculated using potential evapotranspiration corrected by a temperature adjustment factor versus long-term mean temperature. When the soil moisture surpasses a threshold LP, actual evapotranspiration equals potential evapotranspiration. Otherwise, it is calculated as a function of the soil moisture available. All extra water from the soil layer is channeled to the higher reservoir, which is then filled. According to a percolation rate governed by the percolation coefficient PEEC, the latter is drained towards the lower reservoir. The total outflow is the total of the surface flow (Q0), subsurface flow (Q1), and baseflow (Q2), all of which are controlled by the recession coefficients KF, and KS. The KS controls the outflow from the top reservoir on a continual basis, whereas the K0 is only triggered when the water level reaches a KF threshold.

Table 4.2 A range of hydrological parameters of HBV model

Parameter	Description	LB	UB
FC (mm)	Maximum soil storage	1	1000
BETA (-)	Shape coefficient	0.01	6
LP (mm)	Threshold for reduction of evaporation	0.1	1
ALPHA (-)	Measure for non-linearity of flow in quick runoff	0.1	1
KF (-)	Recession coefficient for runoff from quick runoff	0.005	0.5
KS (-)	Recession coefficient for runoff from base flow	0.005	0.5
PERC (min/inch)	Percolation rate occurring when water is available	0.01	10
CFLUX (N/m)	Rate of capillary rise	0	10
WHC (inch)	Water holding capacity of snow	0	1

4.5.1 Hydrological model parameter selection and evaluation

There are different ways of parameter sampling from the upper and lower boundary of hydrological parameters, which depend on the computing times and number of parameters in a specific hydrological model. Beven and Binley (2014) stated that there is no fixed threshold in parameter sampling that varies from ten thousand to a hundred thousand parameter sets. In this study, 30,000 parameter sets were generated from HBV hydrological model parameters range. Characteristics for high flow and low flows have different and need two parallel calibration techniques (Meresa and Romanowicze (2017)).

Meresa and Romanowicze (2017) stated that the NSE likelihood function is relatively useful for high flow simulation due to the interest in peak flow and LogNSE for low flow. In this study, NSE objective function was used to simulate high flow regimes and evaluated against observed streamflow. Based on the model performance, 2000 sets of hydrological model simulations were selected as behavioral conditions.

$$NSE = 1 - \frac{\sum_{t=1}^{j}(Q_{o,t} - Q_{m,t})^2}{\sum_{t=1}^{j}(Q_{O,t} - \bar{Q}_o)^2} \qquad (11)$$

where $Q_{o,t}$ and $Q_{m,t}$ are observed and simulated flow at time t, Q_o is the mean observed flow, and j is the length of the j^{th} time series. The best values of NSE are selected for hydrological model structure and parameter uncertainty analyses.

4.6 Flood frequency analysis

Extreme frequency analysis is crucial to understand the reoccurrence probability of flood events at different return periods. This information plays an essential role in flood control and water resource planning. However, high flow frequency mainly depends on the frequency distribution model type and number of distribution parameters. Depending on the environmental and climatic background, many distributions are deployed in various countries by many researchers to estimate the frequencies of high flow. For example, the Log-Pearson III distribution model is trendy in the USA and Australia for infrastructure design (Griffis & Stedinger, 2007), General Extreme Value and Pearson Type III in Europe (Refsgaard et al., 2013), Gamma and GEV in Africa (Meresa and Getachew, 2018), and Wakeby and Log-Normal distribution types have been frequently used in Asian countries (Chen et al., 2012).

However, one or two statistical distribution model (s) may not capture the entire temporal and spatial variability of hydrological extremes. The most commonly used distribution type (GEV) was applied for flood quantile frequency and magnitude curve development. The distribution was fitted to peak flow to understand the hydrological flood in the selected Upper Awash catchments. In equations (12), the probability density function (PDF) is presented and has three parameters.

GEV $$f(x) = \begin{cases} \frac{1}{\sigma}\exp(-(1+kz)^{\wedge-\frac{1}{k}})(1+kz)^{-1-\frac{1}{k}} & k \neq 0 \\ \frac{1}{\sigma}\exp(-z-exp(-z)) & k = o \end{cases} \quad (12)$$

where α is scale parameter, β shape parameter and location parameter.

4.7 Generalized Likelihood Uncertainty Estimation (GLUE)

The Generalized Likelihood Uncertainty Estimation (Beven and Binley, 1992) approach is widely applied to quantifies the different sources of uncertainty in hydrological flow modeling (Mockler et al., 2016;Bae et al., 2018). This is due to the power of GLUE that is based on Monte Carlo (MC) simulations, and the chosen objective function controls the behavioral condition of the parameter sets. GLUE focuses on reasonable possible solutions generated from the large set of the likelihood of sets using a nominal threshold, which defines the best behavioral condition (Beven & Binley, 2014).

GLUE approach is a non-formal statistical approach that includes Monte Carlos simulations. The hydrological model runs using the entire space of hydrological parameters combination and evaluated using goodness-of-fit criterion (Beven, 2007). Assume likelihood function H(X) to separate the non-behavioral and behavioral simulations produced by different variables X, such as input data, hydrological model parameters, hydrological model structures, and extreme

frequency models. Every i^{th} of the variable X has its own one likelihood measure at time t. The ensemble of each variable Xi (i=1……..m) provides the multi-likelihood measure values H(Xi). The GLUE function is shown in Equation (13). The standard deviation/variance of residual σ2e value is the error in the estimated results affected by the model parameters/input data/hydrological model type/extreme frequency distribution models. If the estimated value of σ2e is near equal to the estimated maximum likelihood or equal to the ration of standard deviation to variance of the observation data σ^2o, the likelihood measure H(X) is equal to zero, which indicates extremely high uncertainty.

$$H(X) = 1 - 1 - \frac{\sigma_e^2}{\sigma_o^2} \quad (13)$$

In this study, GLUE approach was used to estimate the uncertainty associated with hydrological parameters.

4.8 Uncertainty decomposition and estimation

Three main variables, climate models, bias correction techniques, and hydrological parameters, were used to identify the relative uncertainty contribution on the total flood quantile magnitude. Unlike additive or multiplicative uncertainty estimation methods, ANOVA can decompose the aggregated source of uncertainty into individuals' and their interaction using specific extreme flow indices (Meresa and Romanowicz, 2017). Three sources of uncertainty in flood quantile projections that driving from climate models, bias correction methods, and hydrological parameters were estimated using the variances decomposition approach (ANOVA). In this study, n-way of ANOVA was used to distinguish the main variable effects and their interaction effect on the aggregated extreme frequency indices.

$$SST = \sum_{i=1}^{NCM} \sum_{j=1}^{NBC} \sum_{k=1}^{NHP} (Y_{ijk} - \bar{Y})^2 \quad (14)$$

where $Yijk$ is the specific value relating to the climate model i, bias correction methods j and hydrological model parameters k, respectively, and $\bar{Y}$ is the overall mean. The aggregated SST can be further decomposing into three main effects (SS_{CM}, SS_{BC}, and SS_{HP}, the squared deviations of single values from their respective factor mean), which are effects directly attributable to CMs, BCs and HPs, and into three interaction terms (SS_{CMBC}, SS_{CMHP} and SS_{HPBC}):

$$SST = SS_{CM} + SS_{BC} + SS_{HP} + SS_{CMBC} + SS_{CMHP} + SS_{BCHP} + Error \quad (15)$$

where SS_{CM} sum standard error of climate models, SS_{BC} stands for sum standard error of bias correction methods, SS_{HP} sum standard of hydrological parameters, SS_{CMBC} is sum standard error

of combined effect of climate models and bias correction methods, SS_{BCHP} sum standard error of combined impact of climate bias correction methods and hydrological parameters.

4.9 Research Flow Chart

The impacts and uncertainty of projected flood quantile for selected catchments from Upper Awash basin examined using four stages of numerical modeling experiment. The analysis started by selecting natural and/or semi-natural catchments and then extracting, correcting, and evaluating new climate datasets (CMIP6) using three statistical techniques (statistical quantile factor (SQF), distribution quantile mapping (DQM), and Empirical Quantile mapping (EQM)). Then sampling of 30,000 HBV hydrological parameters set using Monte Carlos Simulation (MCS) for hydrological parameter uncertainty estimation using Generalize Likelihood Uncertainty Estimation (GLUE) approach (Beven & Binley, 1992). Finally, generalized extreme value (GEV) was applied to estimate the frequency and magnitude of flood quantile design values.

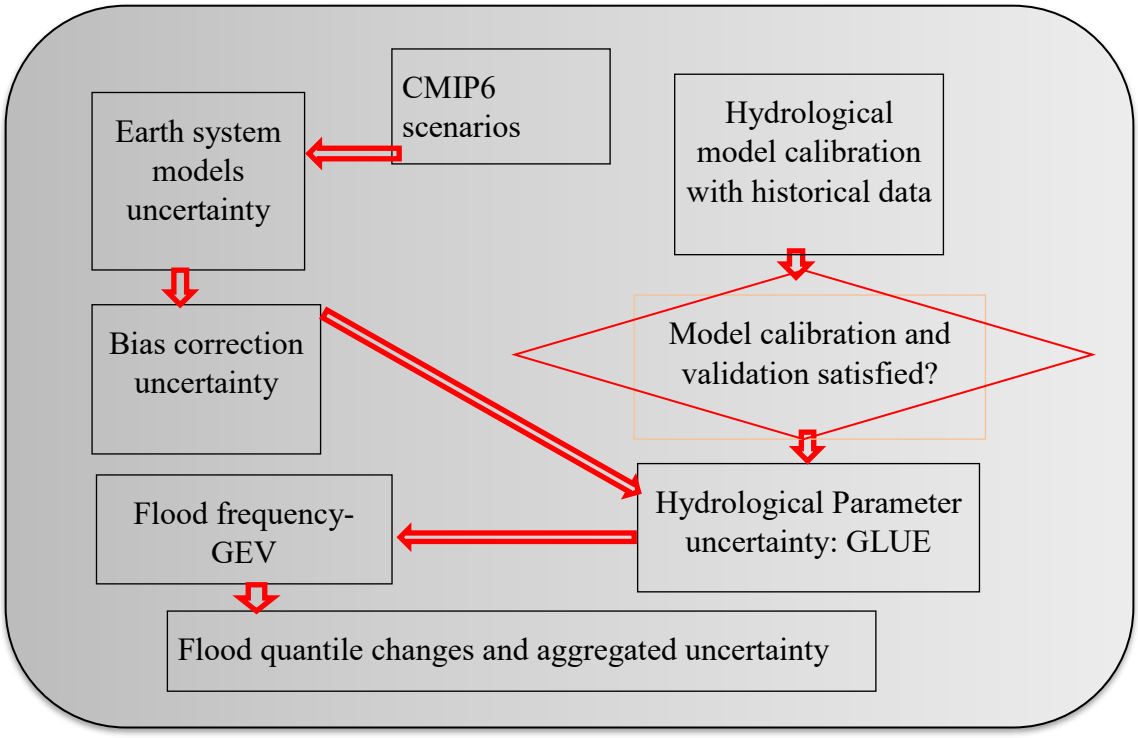

Figure 4.4Research flow chart to estimate projections of flood quantile and identify associated uncertainty

5. RESULT AND DISCUSSIONS

5.1 Evaluation and validation of different climate bias correction techniques

In the first step, the annual maximum precipitation time series of 12 GCMs was evaluated and validated against the annual maximum time series of observed precipitation for 1981-2010. Four statistical matrices were used to measure the accuracy of the annual and seasonal maximum precipitation time series of 12 GCMs in reproducing the daily seasonal and annual maximum time series of observed precipitation.

The results obtained for five catchments in the upper awash basin are presented in Figure 5.1. Overall, the selected stations showed lower MAE, PWRMSE, and PBIAS values, respectively, indicating that the reliability and accuracy of the GCMs precipitation in reproducing observed maximum precipitation is not high. The statistical matrix values were found different for different climate models. The MAE values vary in the ranges of 0.1-20 for annual maximum precipitation, PBIAS values range from -40 to 30, PWRMSE values range from 0 to 0.1, and RR from -0.25 to 0.3 in all the selected catchments. Relatively, the bias correction methods performed better in S1 and S3. This implies that the uncertainty in maximum precipitation is higher than the mean precipitation values. Also, these bias correction methods are also good in reproducing mean precipitation than maximum precipitation values.

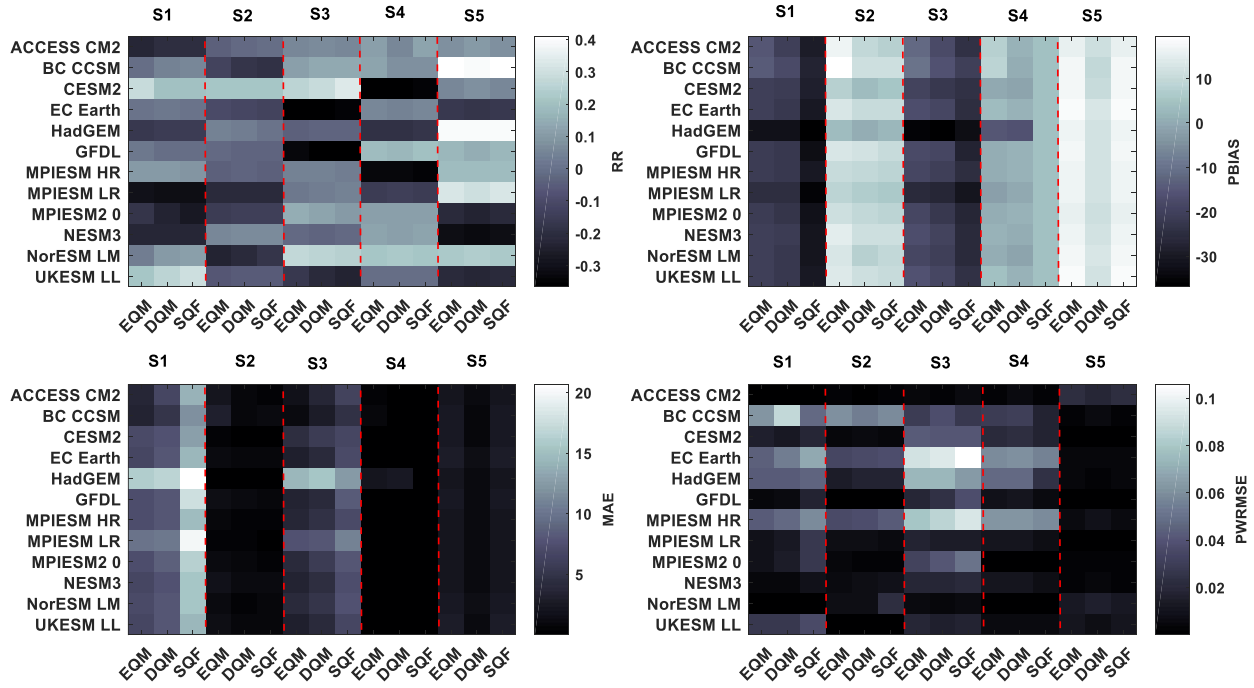

Figure 5.1Comparison of three bias correction techniques with observed daily maximum precipitation using a statistical matrix. The column represents each catchment using three bias correction methods, and each row represents each climate model. S1 stands for Awash Koka, S2 Akaki, S3 Kela, S4 Awash Bello, and S5 Awash Hombole.

The simulated precipitation and temperature from 12 GCMs generally produce biases. Therefore, it is prerequisite to remove these biases before using to force the hydrological model. We used both linear and nonlinear mathematical methods to correct the climate model bias. This helps us to properly capture/corrected different precipitation characteristics. Figure 5.2 shows the comparison of three bias correction methods on simulation of monthly maximum precipitation average over each catchment for the CMIP6 ensemble (color bands, single models shown as a straight line), and the observed monthly maximum precipitation is represented by blue straight-line color for the period 1981-2010. Overall, the 12 GCMs give a broader spread in the rainy season and a relatively narrow band of climate models in the dry season.

The spread of the selected 12 climate model ensemble does not exceed the upper and lower limit of these climate models in the reference period. However, the width of these 12 climate models mainly depends on the type of bias correction method. DQM and SQF methods are relatively given a narrower band/spread than the other. Whereas the EQM provided a wide range of climate model spreads (Figure 5.2). In general, the annual cycle of maximum precipitation shows that the uncorrected GCMs have a considerable bias with respect to observed time series. The result of the three bias correction techniques is not the same in reproducing the observed seasonal maximum precipitation of the selected catchments (Figure 5.2). The performance of these bias correction techniques in the reference period (1981-2010) is uniform in five catchments. The corrected precipitation range/band of 12 climate models is relatively smaller using distribution quantile mapping and empirical interpolation.

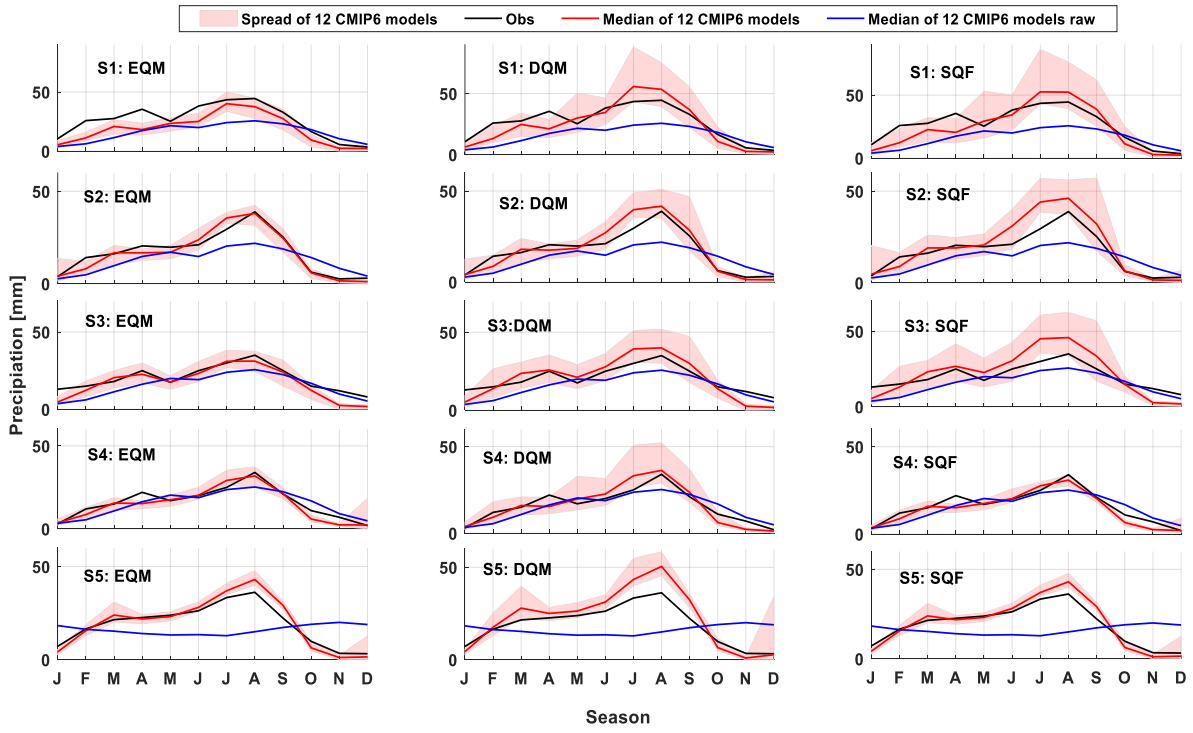

Figure 5.2 Comparison of seasonal raw and bias corrected daily maximum precipitation simulations from 12 CMIP6 GCMs for each of five study catchments. Each column presents results of one bias correction method of five catchments. Each row presents a result of three bias correction methods of one catchment. In each panel the shaded area represents the range of 12 GCMs, and blue line is the raw median of raw 12 GCMs with black line the observed seasonal maximum precipitation. S1 stands for Awash Koka, S2 Akaki, S3 Kela, S4 Awash Bello, and S5 Awash Hombole.

These climate bias correction methods were applied to each GCM in the future period (2015-2100). The influence of each climate bias correction method on the magnitude of change was assessed (Figure 5.2). Daily precipitation between 2040-2069 (near future - clim2) and 2070-2099 (far future - clim3) was compared to the reference period 1981-2010. An increase was simulated in the far and near-future period by all climate scenarios in terms of annual maximum precipitation.

Similarly, changes from each bias correction approach show a slight difference in magnitude and direction in changing annual precipitation. For example, in catchments Awash Koka and Awash Hombole shows a higher change in annual maximum precipitation in all the bias correction, -10 to 300%. Whereas, the other catchments show -10 to 100% change in extreme precipitation. Moreover, the changes are smaller in Awash Koka and Awash Bello using DQM methods, whereas in Akaki and Kela changes are smaller using EQM and DQM.

The climate change signals are also indicating a higher change suing SSP5-85 scenario than SSP3-70 and SSP1-26 in the all the catchments due to higher emission radiation value in SSP5-85 than the other scenarios (SSP1-26 and SSP3-70). Interestingly, there is a linear relationship between the annual maximum precipitation changes in clima1 and clima2 with proportional magnitude. This indicates that the slope of these changes in clim1, clim2, and clim2 is a positive trend.

Figure 5.3 shows the projected maximum air temperature under each SSP scenario for each of the 12 climate models, together with the mean of the ensemble air temperature projected for each SSP. Daily air temperature is more stable and consistent with time and space in Ethiopia (Meresa and Getachew, 2018). The projected air temperature from the new climate dataset and new scenarios provides reasonable temperature change, increasing by 1.9-3.5^{o}c and relatively uniform in the selected catchments. However, the spreads of the selected climate models are more extensive in Awash Koka and Awash Hombole. Overall, the projected air temperature has a positive slope and continuously increasing in the clim1, clim2, and clim3 future period.

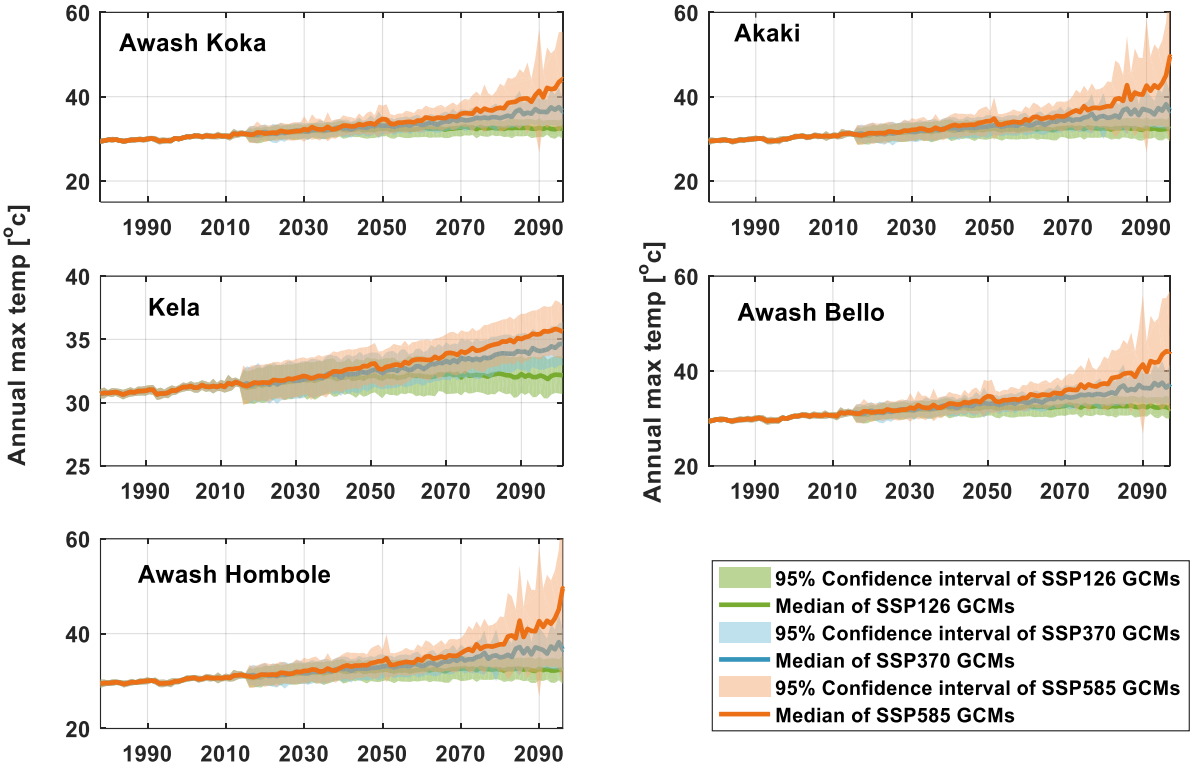

Figure 5.3 Ensemble of 12 climate models of mean air temperature projections for the period 1975-2100. The orange, Blue, and Green shaded areas stand for the spread of SSP5-85, SSP3-70, and SSP1-26 scenarios, respectively. The solid lines represent the 12 climate models' median for each scenario – red for SSP5, blue for SSP3, and SSP1.

5.2 Hydrological modeling and parameter uncertainty evaluation

The HBV hydrological parameter sets (for each of nine HBV parameters) with a sample size of 30,000 were generated through uniform distributions. GLUE-based parameter uncertainty approach was adopted to simulate a possible ensemble of daily streamflow, and NSE objective function was applied to separate the behavior and non-behavior simulations. In this study, the runoff simulation ensemble with likelihood value larger than 0.3 NSE threshold value was selected. The likelihood value less than the NSE threshold value of the HBV parameter sets is considered as non-behavioral. Figure 5.4 shows the HBV hydrological model performance in the reference period.

Hydrological model is very helpful to understand the catchment processes. However, due to lack of accurate mathematical representation of the real work, all hydrological models need to calibrate using the observed streamflow. The HBV model calibration in the upland Awash river basin: at the upper Koka, Melka Hombole, Awash Bello, and Akaki catchments, showed that model performance capabilities in reproducing the observed streamflow were good or higher.

The NSE were used as objective function. The comparison was performed at daily time steps and had a favorable comparison during all the five sub-basins (Figure 5.4). This is evident from the optimal values of NSE varied from 0.59 to 0.83. The NSE values of upper Koka is 0.83, Melka Hombole 0.72, Awash Bello 0.59, and Akaki 0.65 catchments during the calibration period. After the model was calibrated, an independent dataset that was different from the calibration periods was used to validate the model at the chosen River Basin, with no further changes to the calibrated parameters. The HBV model has been found to have a very good predictive capability with NSE objective function value ranging from 0.53 to 0.88, and has a value of 0.61, 0.56, 0.79, 0.88 and 0.62, respectively, for a daily basis.

The model performance is not uniform across the selected catchments due to the differences in hydroclimatic characteristics. Especially, the lower recession of the hydrograph, the model lacks in all the catchments. This is mostly due the significant role of physiographic condition of the catchments. However, the conceptual hydrological model is highly capable to simulation high flow, but not application for low flow simulations, which is the main objective of this thesis (on projections of high flow). In general, the daily peak flow predictions differed between the two catchments when compared to the observed stream flow. During the calibration and validation time, underestimation of daily peak values was recorded for the Akaki sub- catchment, while minor overestimation occurred during the small rain season. In both seasons, the predicted flow for the Hombole catchment overestimated some of the daily peak flows (Figure 5.4 and Figure 5.5).

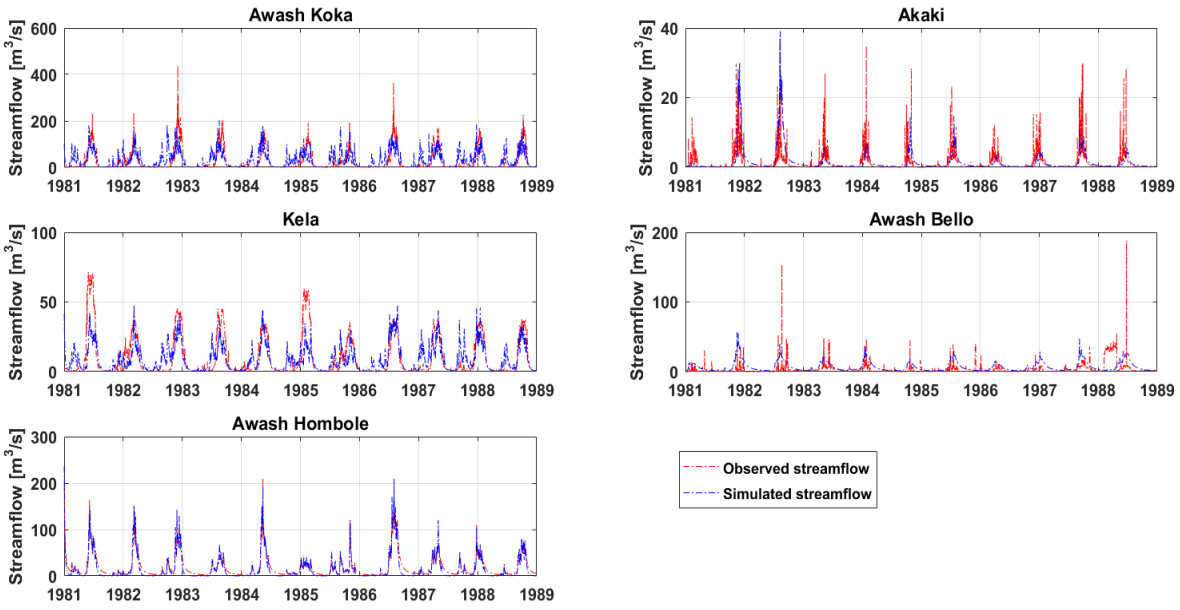

Figure 5.4 HBV hydrological model performance in the calibration period using the NSE objective function.

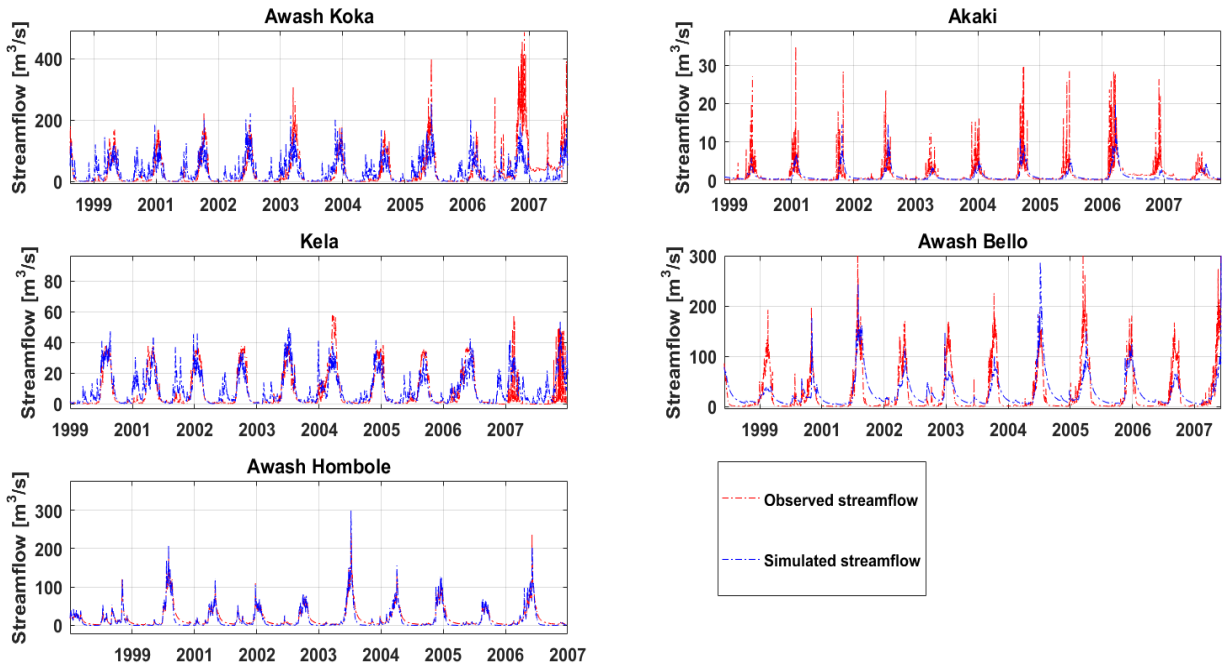

Figure 5.5 HBV hydrological model performance in the validation period using the NSE objective function.

The soil moisture routine (Bergström, 1976) uses the excess precipitation to compute soil moisture storage, infiltration, and percolation through the soil. The parameter FC determines the soil's maximum storage capacity (FC). The ratio between actual soil moisture and FC is used to calculate infiltration. BETA is a parameter that compensates for variable soil infiltration properties. Even when soil moisture is low, the smaller the BETA, the more water is transferred to the following procedure compared to FC. Actual evaporation is calculated as a function of the parameter LP (fraction of soil moisture storage above which actual evaporation should equal potential evaporation). For runoff generation, a single linear reservoir model is used. It's a straightforward catchment model in which runoff is considered to be proportionate to soil water storage at any given time.

Table 5.1 is the result of optimal HBV hydrological model parameters. These are values related to the median of the 30,000 generated parameters using GLUE-MC simulation. The focus was mainly to estimate the uncertainty rather than sensitivity of the model parameters. However, When the emphasis is on high flow simulation (i.e., using NSE fitting criteria), the model parameters FC, ALPHA, and BETA have the highest sensitivity values (based on the values range); and when the emphasis is on low flow simulation (i.e., using logarithm transformation of flow NSE fitting criteria), the HBV model parameters FC, PERC, and KS have the highest sensitivity values. In general, the most sensitive parameters in all stations chosen as case studies were and FC. and FC were both part of the soil module, and they reflected soil moisture variation,

nonlinear routing, and respectively. Furthermore, in mountainous catchments, the surface runoff component and soil moisture processes were the most dominant.

Table 5.1. Optimal parameters of HBV hydrological model using NSE objective function

CODE	S1	S2	S3	S4	S5
River/Lake	Awash_K	Akaki	Kela	Awash_B	Awash_H
Guage at site at/Nr	U/Sof Koka	Aba S	Welen	Bello	Melka H
FC	1254	712	640	480	875
LP	0.282	0.72	0.901	0.8105	0.438
BETA	1.226	1.993	0.85	1.4215	0.767
PERC	0.738	0.944	0.902	0.923	0.206
ALPHA	1.309	3.184	0.01	1.597	1.875
KF	0.008	0.081	0.01	0.0455	0.073
KS	0.037	0.074	0.15	0.112	0.037
CFLUX	1.767	2.991	1.35	2.1705	1.224
WHC	0.26835	0.49935	0.20865	0.354	0.231

5.3 Performance of hydrological models under different bias correction approach

The changes in flow simulations forced using three bias correction climate variables have been compared and presented in Figure 5.6. Overall, it observed positive changes in annual maximum flow using DQM, EQM, and SQF, 10%, 17%, and 23% respectively in Awash Koka. However, there is a slight difference among these bias correction techniques. For example, SQF shows a smaller change in peak flow in Awash Bello (12%) and Awash Hombole (16%) catchments, whereas as, in catchment Awash Koka (23%) and Akaki (35%) shows a higher change in peak flow.

Generally, the magnitude of annual maximum flow changes is not the same. However, these are not uniform across the selected catchments, bias correction methods, and climate scenarios. Relatively, distribution-based bias correction models give smaller changes in the annual maximum flow time series. This indicates that wet-day frequency correction that considered in DQM is significant in understanding the future maximum flow projections. Mainly, annual maximum flow changes using EQM give a higher spread range and uncertainty. Boldly observed that annual maximum flow changes have smaller uncertainty (size of the box plot) in SSP370 and higher in SSP126 (Figure 5.6).

Therefore, correcting the wet-days and intensity of precipitation may significantly change the change magnitude and direction and minimize uncertainty.

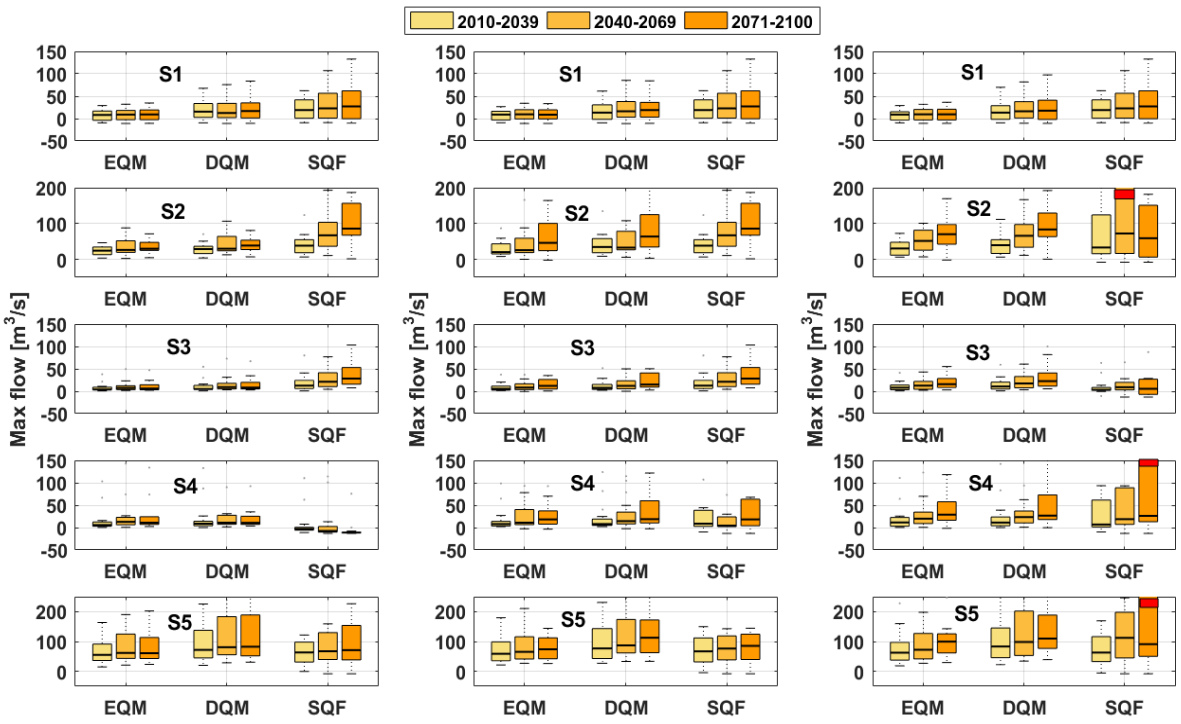

Figure 5.6 River flow change in clim1 (2010-2039), clim2 (2040-2069), and clim3 (2071-2100) with respect to the reference period (1981-2010). Each box plot represents the spread of twelve climate models listed in Table 4.3 with median 0.5 and 0.25 and 0.75 quantiles. Each column stands for each scenario (the first column for SSP126, the second column for SSP370, and the third column for SSP585). Each row represents each catchment (first row S1- Awash Koka, second row S2- Akaki, third row S3- Kela, fourth row S4- Awash Bello, and the last row for S5- Awash Hombole). The red box at the top of the both in the right side indicates extreme outlier points.

5.4 Flood quantile projections under varying climate conditions

The projected annual maximum series has different distribution characteristics, resulting from different flood quantile magnitude and risk level. Of which, the three most dominant and best-fitted distribution models have similar probability density functions (PDF). Using the most dominant PDF model (GEV), the flood quantile changes due to climate change have been evaluated. Figure 5.7 shows flood quantile changes in climate1 clim2 clim3 with respect to the reference period, estimated using an ensemble of 12 GCMs and three bias correction methods. The ensemble average of 12 climate models within three scenarios assessed (SSP1-26, SSP3-70, and SSP5-85) and three bias correction methods in five catchments show a significant increase in flood quantile magnitudes and frequency in the future (Figure 5.8). Mostly, the changes of

flood quantiles are consistent with changes in maxima flow, but it does not mean that the magnitude of changes and directions are the same. The future flood quantile changes are not the same in space and bias correction methods, and the frequency of the larger return period flood increases to higher than once in 20 years. The smallest changes are observed in Awash Koka using EQM, Awash Bello using SQF, S5 using DQM, and S3 using EQM. Relatively the methods are consistent in Akaki and Kelo in providing information about flood quantile changes in the future. Simultaneously, with different hydro climatic simulations, the flood quantile changes are significant at different return periods. For example, Awash Koka catchment has a change range from 0-100% but using the DQM; the changes range from 0-170%. Similar ly, in Awash Hombole catchment 0-100% using DQM.

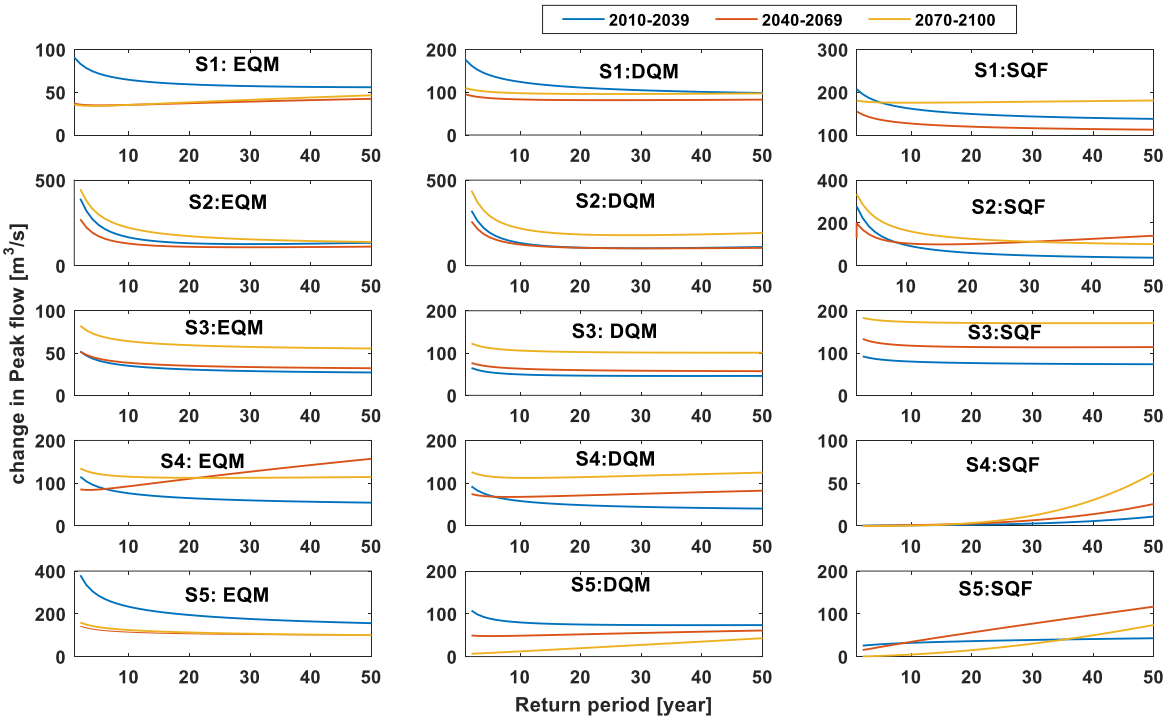

Figure 5.7 Changes in peak flow quantiles using three bias correction techniques and GEV frequency distribution model at each catchment. First column (climate inputs with EQM correction; second row) climate inputs with DQM correction; and third row) climate inputs with SQF correction. S1 stands for Awash Koka, S2 Akaki, S3 Kela, S4 Awash Bello, and S5 Awash Hombole.

5.5 Uncertainty estimation and decomposition of associated sources in flood quantile estimation

The three sources of uncertainty were estimated based on the one chain principle. The one chain uncertainty band quantification started from one climate model that passed through three bias correction techniques and the best hydrological parameters (Figure 5.8). The contribution of each source of uncertainty is not uniform across the selected catchments. Each color band represents each source of uncertainty as a relative range of cascade uncertainty. Spreads of the 12 climate

models represent the climate models uncertainty band; the hydrological parameter uncertainty is presented by 95% confidence interval of selected hydrological parameter sets. The uncertainty due to bias correction types are estimated from the spread of three bias correction simulation results is estimated. However, the ensemble uncertainty of GCMs is relatively more considerable than the other sources. Whereas hydrological parameter sets do not play a significant role in future quantile estimation (Figure 5.8). Future flood quantile in Awash Koka catchment is highly sensitive to climate change and respective bias correction methods. Whilst Akaki catchment is more sensitive to distribution model and bias correction methods in flood quantile estimation.

Figure 5.8 shows only the main sources of uncertainty (hydrological parameter sets, climate models, bias correction methods, and frequency distribution models) and their respective bands at specific return periods and catchment, with considering the main factors' interdependence using ANOVA, the contribution of individual sources of uncertainty as the main source and their interaction contribution to the flood quantile magnitude and frequency changes in future. The decomposition of source uncertainty from the main variables and their interaction were separated based on the variance in flood quantile values and calculated out of 100, which means the sum of all sources is 100. The role of hydrological parameter sets on flood quantile projection is not significant and less uncertain in the selected catchments. In comparison, the climate change variability shows a significant impact and uncertainty on the projection of flood quantile. This may be due to the projected precipitation intensity, higher temperature, and concentration time in the area. On the other side, the contribution of hydrological parameter sets is not significant in flood quantile estimation. Floods are not dominated by hydrological processes like ground and interflow (Figure 5.8). In general, the dominant source of uncertainty is climate models, and the hydrological parameter sets related uncertainty is not significant source of uncertainty in future flood design value estimation. The share of climate models, bias correction, and frequency distributions are significant at design flow value estimation at 100 return period. In Awash Koka, future flood quantile risk is highly uncertain due to climate model variability and their respective bias correction methods. Whereas Akaki catchment is more sensitive to the frequency distribution and climate model variability.

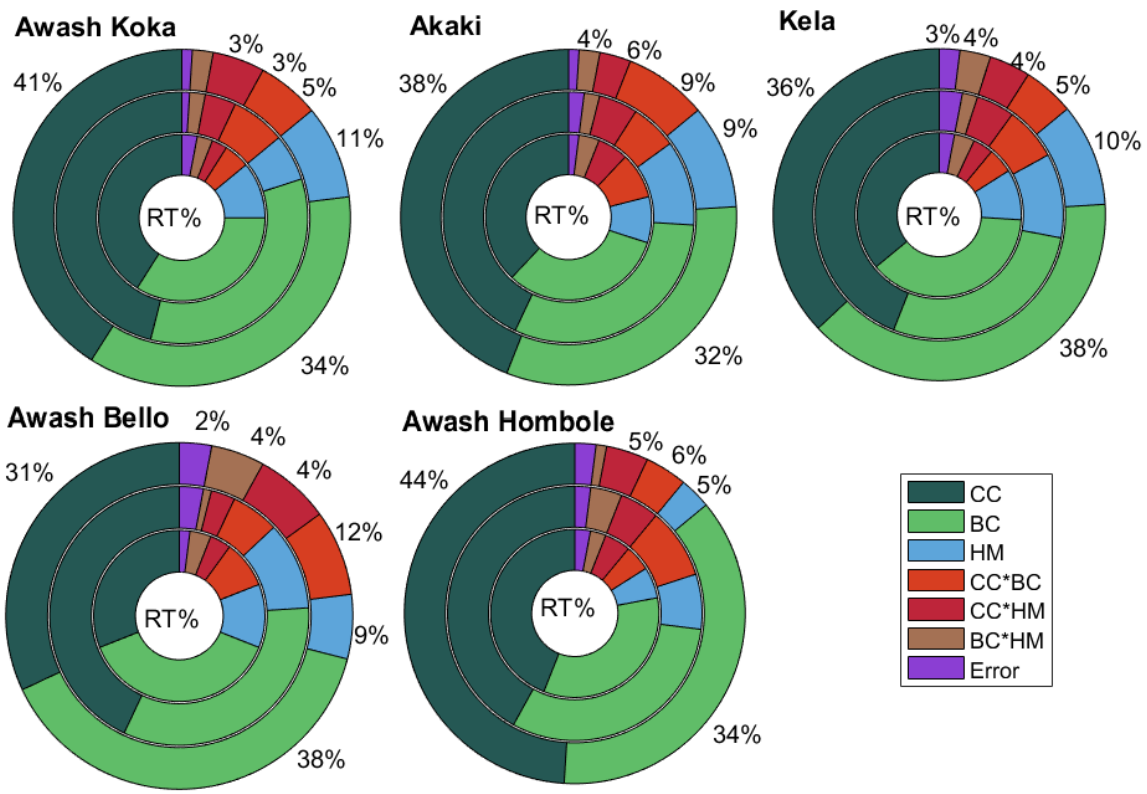

Figure 5.8 Contribution of each source of uncertainty in flood frequency estimation under climate change. The three circles present flood quantile results at RT=20 yrs, RT=50 yrs, RT=100 yrs from inside to outside, respectively. Each color represents each source of uncertainty: dark green is uncertainty from climate models (CC), light green from bias correction methods (BC), and Blue color from hydrological parameters (HP), and the other colors represent the interaction between the main factors.

5.6 Discussion

5.6.1Projected hydro climatic variables using CMIP6 scenarios

In this study, CMIP6 climate change dataset source was used to understand the impact and uncertainty in future flood quantiles. From CMIP6 GCMs, 12 GCMs climate models with three climate scenarios (SSP126, SSP370, SSP585) was applied for future hydrological extreme simulations. Due to the lack of robust atmospheric-land model interaction, uncorrected GCMs do not recommend to use for extreme hydrological modeling (Meresa et al., 2017;Mendez et al., 2020). However, the impact of climate change magnitude also depends on the bias correction methods' principles (Pierce et al., 2015). Three climate bias correction methods were applied to correct the GCMs output with daily observed air temperature and precipitation. Overall, from the three bias correction methods used, the distribution base was enabled to reproduce the observed maximum precipitation. This implies that correction of wet-days and intensity of GCMs is

significant and provides a significant role in minimizing uncertainty. Whereas the air temperature is corrected using the empirical methods and gives a similar result without a considerable difference in reproducing the daily mean air temperature. This shows that the magnitude mainly depends on the type of methods and significantly influences the magnitude of maximum precipitation changes.

Moreover, the maximum precipitation and air temperature will increase and decrease in the coming decades using CMIP6 data and varies with time and space. Each climate model in each scenario gives a different direction and magnitude. The highest change in annual maximum precipitation was observed in Awash Bello catchment, whereas, in Awash Hombole the changes in the clim2 and clima2 show a non-significant (near to zero) magnitude and direction. In Awash Koka catchment, most climate models indicate a positive change, but these changes are very small. These changes in precipitation and air temperature are consistent with previous findings using RCP-AFRO-CORDEX (Meresa & Gatachew, 2018b;Taye et al., 2015), using MIROC-ESM-CHEM and CSIRO-Mk3-6-0 (Daba et al., 2020), and using Statistical Down-Scaling Model, SDSM-CMI5 (Gebrechorkos et al., 2020) in Ethiopia.

The annual daily maximum precipitation and daily mean air temperature projected under SSP1-26, SSP3-70, SSP5-85 shared socioeconomic pathways scenarios suggests that wet conditions could be slightly intensified and increased in Awash Koka and Awash Hombole by more than 50%, 80% and 120%, respectively.

However, it doesn't mean that the entire maximum precipitation produce flood in all area, the mean peak flood is not higher in the normal condition. In contrast, the magnitude of the positive changes in maximum precipitation will be intensified in Awash Koka and Akaki, ranging from 30-95%. Similarly, the mean temperature changes of these selected catchments are not much different in magnitude and direction, and the changes are lies in the range 1.9 and 3.5^{o}c. However, SSP1-26 gives lower changes in precipitation and temperature magnitude than changes using SSP3-70 and SSP5-85.

5.6.2 Modelling and projections of hydrological extremes using CMIP6 dataset

Five catchments have been selected from different hydro climatic and geographical locations to determine the impact of climate change on flood quantile and identify the associated uncertainty in the projected flood quantile magnitude and frequency. HBV hydrological model was calibrated and validated against the observed streamflow data using Nash-Sutcliffe (NSE) objective function (performance measure) in the period of 1981-1990 and 1991-2005,

respectively. NSE value higher than 0.5 indicates a satisfactory hydrological simulation zone (indicates how well the hydrological model reproduces the extremely high flow) (Bennis & Crobeddu, 2007) and promising for further analysis. The five catchments have an NSE value ranging from 0.5 to 0.75 from 30,000 parameter sets. Of which, NSE value 0.5 was selected as a threshold in runoff simulation and accepted for future runoff simulations. Similarly, other studies also show similar results using HEC-HMS (Roth et al., 2018), using SWAT model (Shawul et al., 2019), and using HBV light model (Bekele et al., 2019) in Awash catchments.

Uncorrected and the future corrected precipitation and temperature data from CMIP6 data sets were used to force the HBV hydrological model and to examine the potential impact of climate change on the future flood quantile/peak flow. Overall, the projected high flow changes are positive, which is an increase in high flow in the near future (2010–2039), far future (2040–2069), very far future (2070–2099) for an ensemble of SSP3. Like the precipitation changes, the effect of climate bias correction on high flow change is clearly visible and brought higher changes in magnitude with a large uncertainty band. However, the distribution-based quantile mapping techniques relatively produce reasonable changes in high flow at the selected sites. The changes are higher using SSP1-26 and SSP5-85 climate scenarios.

In contrast, the SSP3-70 gives a smaller band in high flow changes in a near and far future period, which is a direct reflection of maximum precipitation change. In S1 and S4 catchments, the near future changes, far future, very far future for an ensemble of SSP370 shows significant changes with a large uncertainty band. Whereas in S2 and S3 catchments, the changes are not uniform across the bias correction methods, and changes are smaller than S1. This is most likely due to increased summer and spring precipitation (Meresa and Getachew, 2018). Similarly, the distribution-based climate bias correction gives relatively smaller comparisons with the empirical and linear interpolation methods at most of the catchments.

5.6.3 Flood quantile estimation under climate change

The impact of climate change on flood quantiles was assessed through the extreme frequency distribution models. The baseline and future flood frequency simulations of each catchment were estimated from 12 climate models (GCMs). Various distribution types are commonly used in the US, Europe, and Africa (Kay et al., 2009; Collet et al., 2017; Meresa & Romanowicz, 2017; Meresa & Gatachew, 2019; Lawrence, 2020). In this study, the most dominant flood frequency model was selected for flood quantile estimation. GEV distribution model were applied for flood quantile estimation and associated impacts. The estimated magnitude of flood quantiles at

different return periods using GEV frequency distributions is not the same in magnitude and uncertainty band. Each climate model at each catchment gives a very wide range of flood quantile values. Overall, smaller flood quantiles were observed in S3 catchment, whereas the highest was estimated from S1 and S4 catchments. The estimated quantiles' total range is relatively smaller in S3 and S2, whereas the highest uncertainty range is estimated on S4 and S1 catchments.

Moreover, the changes of flood quantile values are not the same (significance difference) across the catchment and type of bias correction methods. In the S2 and S3 catchment, the flood quantiles at different return periods are expected to be larger in the near, far, very far future. In comparison, the changes are relatively higher in S1 and S4 catchments and expected to be higher in the very far period. This is mainly due to the magnitude and distribution of flood events in the given period (Armstrong et al., 2012; Keast & Ellison, 2013).

5.6.4 Projected Flood quantile associated Uncertainty estimation and decomposition

In this study, 12 climate models, three bias correction methods, HBV hydrological model with 30,000 parameter sets, GEV flood frequency model, and three climate scenarios from the new dataset (CMIP6) were considered to analyze the impact of future flood quantile in the selected five upper awash catchments. Using additive uncertainty aggregation, each component of these analyses is integrated into one framework that contains information from each part. Climate models highly uncertain in characterizing the future climate variables.

In the last decades, the various study stated that RCP and SRES climate scenarios outputs are very weak in reproducing the historical climate extremes (Fowler et al., 2007; Kingston et al., 2011;Saini et al., 2015; Meresa & Romanowicz, 2017). This uncertainty is may be due to the structure, parametrization, and spatial resolution of the GCMs. Using multiple models in climate change impact analysis would lead to an improved understanding of the uncertainty associated with climate models. It is essential in flood risk magnate and water resource management. Similarly, in this study, multiple climate models from the new data set CMIP6 (shared socio-economic pathway scenarios) were evaluated for flood quantile projection in upper awash basin and found that the spread/discrepancy of climate models' impact is significant.

There are also important uncertainties component which is associated with the climate bias correction methods. The catchment-scale characteristics are not the same as the GCMs spatial and temporal characteristics; therefore, it is important to use highly relevant climate bias correction techniques to understand the uncertainty and minimize. Three bias corrections were effectively corrected in the historical period and then adopt the parameters for future climate

corrections. There are few studies related to bias correction methods uncertainty and flood frequency (Kay et al., 2009; Saini & Roop, et al., 2015; Soriano, et al., 2019). They found that the climate bias correction could alter the magnitude of flood quantile. This study also confirmed this study using three climate bias correction methods and GCMs from CMIP6 in Ethiopia's selected catchment. We find that the uncertainty source due to wet-days and intensities of precipitation has a significant impact on the flood quantile magnitude (e.g. S4 catchment).

The hydrological model structure and parameters represent hydrological process. The hydrological parameters control the flow from single droplet of rain to the deep catchment percolation. In this study, more sensitive parameter sets of HBV hydrological model were selected using NSE objective function values (0.5 as threshold). GLUE was used to investigate the role of hydrological parameters in flood quantile estimation in the selected catchments. The analysis was performed by using a uniform sampling approach from the given HBV parameter ranges. The ranges of the HBV were procured from Meresa & Gatachew, (2019). The simulated flow in the historical period is pretty good for mean and high flow simulation. The width of the simulated band is not significantly increased by changing the threshold for high flow simulation. Generally, the uncertainty due to hydrological parameter change is not significant in flood quantile estimation. The result confirmed that hydrological parameter sets' role is less in all the selected catchments in upper awash basin. Yan et al., 2015;Meresa & Romanowicz, 2017;Joseph et al., 2018 they appear with similar conclusion that high flow is less sensitive to hydrological parameters.

The uncertainty related to flood frequency under climate change is not extensively investigated and it has been very challenging to integrate with other sources of uncertainties. Each extreme high flow simulation from each climate model simulation and bias corrected simulations were fitted to most dominant frequency models. several researchers have been conducted flood frequency estimation, and they concluded that GEV and extreme value (EV) distribution models are the most commonly used frequency models in Awash catchments (Ahilan et al., 2012). However, numerical experiment result confirms that GEV distribution is the most dominant type of model in the selected upper awash catchments. The uncertainty band is not significant in the selected catchments of flood quantile values. Therefore, the uncertainty of flood frequency models in these catchments is avoidably in the hydro-climate projections. The results should be counted with care because the probability of recurrence of extreme floods of the selected catchments are become more intense and frequent and intense in the near, far, and very far future periods.

6. CONCLUSIONS AND RECOMMENDATIONS

6.1 Conclusions

The results of climate variables from CMIP6 data set are consistent with previous studies and applied for the first time in estimation of future flood quantile under varying climate conditions and associated uncertainty estimation. The results also prove that the need for proper bias correction technique can improve in reproducing observed precipitation and temperature characteristics. The climate models bias is corrected using three techniques (DQM, EQM, and SQF). The precipitation results using the DQM approach are relatively close to observed daily maximum precipitation data. This indicates that climate models have higher biases in projection of extreme precipitation magnitude (greater than 75% of the maximum precipitation), and smaller bias results in lower precipitation magnitude (lower than 75% of the maximum precipitation). This is due to seasonal variability and intensity of precipitation. Therefore, giving more focuses to upper quantile of precipitation distribution can improve the model's capability in reproducing the observed time series and reducing uncertainty related to precipitation and temperature.

The projected hydro-climate extreme indices are less consistent and indicate a strong model agreement with a wide range of variability in the selected catchments. However, the magnitudes of changes in hydro-climate extreme indices are mainly depending on the type of bias correction technique. DQM, EQM, and SQF give relatively smaller range of changes in annual maximum precipitation and annual maximum flow. Overall, increases in flood and extreme rainfall are expected and are not uniform in space/time. Similarly, the GEV frequency model was fitted to simulated annual maximum flow time series. The flood quantile changes were calculated based on the relative difference between the future (2015-2100) and historical (1981-2010) flood quantile simulations. Due to precipitation and temperature changes, the magnitude of flood quantiles at different return periods between 5 to 100 years could increase between 5% and 50% in the selected catchments in the 21st century. However, these changes are not the same across all bias correction methods and frequency models in each catchment.

The uncertainty analysis was performed by comparing each source of uncertainty regarding the total aggregated value flood quantile at different return periods. The result confirms that hydrological model parameters spread of climate models and bias correction techniques are important sources of uncertainty in flood quantile estimation. Specially, the climate models, bias correction methods and frequency distribution type models are the most significant source of uncertainty in future flood quantile estimation. This additive of uncertainty analysis is also

proved by ANOVA analysis. ANOVA is variance-based sensitivity analysis and provides information about the main factors' contribution and their interactions.

The decomposition of source of uncertainty in future quantile estimation was performed based on the variance in changes of flood quantile value at Q20 (probability of recurrence of flood event at 20 years return period), Q50 (probability of recurrence of flood event at 50 years return period) and Q100 (probability of recurrence of flood event at 100 years return period). The result confirms that climate change is the dominant factor in Awash Koka and Akaki, whereas S3 bias correction type and Awash Bello distribution type are very important factors. ANOVA also confirms that the contribution of their interactions is significant.

6.2 Recommendation

For the coming 90 years, the discharge values (floods) of the same return period may be more relatively the current climate condition; and more likely urban flooding (street flooding) due to increased rain fall may occur. Therefore, there is a need to modify urban infrastructure design criteria (for example take in to account the climate change impact for design of culvert in the city).

This study involved a number of models and model outputs where each possessed a certain level of uncertainty. Hence, the results of this study should be taken with care and be considered as indicative of the likely future rather than accurate predictions. Meanwhile, this study should not be extended by considering changes in land use, soil and other climate variables.

The model simulation considers only the climate variable by assuming all other thing constant. But change in land use and soil management activities will also contribute great impact on rain fall runoff process of the watershed. Therefore, future research should be focus on land use land cover change including climate change.

The contribution of climate models and bias correction methods and interaction is especially substantial and no negligible in flood quantile estimation. Moreover, better flood risk management and policy need to consider these main factors and their management policy interaction. The value range of each source is large and challenging to communicate with decision-makers and stakeholders. Therefore, I strongly recommended considering the use of each spread's median values for future flood risk management and take as standard information on extreme flood adaptation measures.

REFERENCES

Ahilan, S., O'Sullivan, J. J., & Bruen, M. (2012). Influences on flood frequency distributions in Irish river catchments. Hydrology and Earth System Sciences, 16(4), 1137–1150. https://doi.org/10.5194/hess-16-1137-2012

Ali, K., Ahilan, S., O'Sullivan, J. J., & Bruen, M. (2012). Influences on flood frequency distributions in Irish river catchments. Hydrology and Earth System Sciences, 16(4), 1137–1150. https://doi.org/10.5194/hess-16-1137-2012

Ali, K., Bajracharya, R. M., & Koirala, H. L. (2016). A Review of Flood Risk Assessment. (May 2018). https://doi.org/10.22161/ijeab/1.4.62

Allen, M., and Ingram, W. (2002). Constrains on future changes in climate and the hydrologic cycle. Journal of Nature, 419, 224-232.

Almazroui, M., Saeed, F., & Saeed, S. (2020). Projected Change in Temperature and Precipitation Over Africa from CMIP6. July. https://doi.org/10.1007/s41748-020-00161.

Al-Safi, H. I. J. & Sarukkalige, P. R. 2017 Assessment of future climate change impacts on hydrological behavior of Richmond River Catchment. Water Science and Engineering 10 (3), 197–208. https://doi.org/10.1016/j.wse.2017.05.004.

Armstrong, W. H., Collins, M. J., & Snyder, N. P. (2012). Increased Frequency of Low-Magnitude Floods in New England. Journal of the American Water Resources Association, 48(2), 306–320. https://doi.org/10.1111/j.1752-1688.2011.00613.

Aven, T. (2019). Climate change risk–what is it and how should it be expressed? Journal of Risk Research, 0(0), 1–18. https://doi.org/10.1080/13669877.2019.1687578

Badilla, R. a. (2008). Flood Modelling in Pasig-Marikina River Basin. Modern Applied Science, 8(5), 1–73. https://doi.org/10.5539/mas.v8n5p80

Bae, D. H., Trinh, H. L., & Nguyen, H. M. (2018). Uncertainty estimation of the SURR model parameters and input data for the Imjin River basin using the GLUE method. Journal of Hydro-Environment Research, 20(October 2016), 52–62. https://doi.org/10.1016/j.jher.2018.05.001

Balke, T., & Nilsson, C. (2019). Increasing Synchrony of Annual River-Flood Peaks and Growing Season in Europe. Geophysical Research Letters, 46(17–18), 10446–10453. https://doi.org/10.1029/2019GL084612

Bastola, S., Murphy, C., & Sweeney, J. (2011). The sensitivity of fluvial flood risk in Irish catchments to the range of IPCC AR4 climate change scenarios. Science of the Total Environment, 409(24), 5403–5415. https://doi.org/10.1016/j.scitotenv.2011.08.042

Beck, H. E., A. I. J. M. van Dijk, and A. de Roo (2015), Global maps of streamflow characteristics based on observations from several thousand catchments, J. Hydrometeorol., 16(4), 1478–1501.

Bekele, D., Alamirew, T., Kebede, A., Zeleke, G., & Melesse, A. M. (2019). Modeling Climate Change Impact on the Hydrology of Keleta Watershed in the Awash River Basin , Ethiopia.

Beigi, E., Tsai, F. T. C., Singh, V. P., & Kao, S. C. (2019). Bayesian hierarchical model uncertainty quantification for future hydroclimate projections in Southern Hills-Gulf region, USA. Water (Switzerland), 11(2). https://doi.org/10.3390/w11020268

Bennis, S., & Crobeddu, E. (2007). New runoff simulation model for small urban catchments. Journal of Hydrologic Engineering, 12(5), 540–544. https://doi.org/10.1061/(ASCE)1084-0699(2007)12:5(540)

Berg, P., Feldmann, H., & Panitz, H. J. (2012). Bias correction of high resolution regional climate climate model data. Journal of Hydrology, 448-449,80-92.https://doi.org/10.1016/j.jhydrol.2012.04.026

Bergstrom, S. (1992). The HBV model: Its structure and applications. Swedish Meteorological and Hydrological Institute, Norrkoping.

Bergström, S. (1976). Development and Application of a Conceptual Runoff Model for Scandinavian Catchments. Smhi, RHO 7(November), 134. https://doi.org/10.1007/s11069-004-8891-3

Beven, K., & Binley, A. (1992). The future of distributed models: Model calibration and uncertaintyprediction.ydrologicalrocesses,6(3),279–298.https://doi.org/10.1002/hyp.3360060305

Beven, K. (2007). Towards integrated environmental models of everywhere: Uncertainty, data and modelling as a learning process. Hydrology and Earth System Sciences, 11(1), 460–467. https://doi.org/10.5194/hess-11-460-2007

Beven, K., & Binley, A. (2014). GLUE: 20 years on. Hydrological Processes, 28(24), 5897–

5918. https://doi.org/10.1002/hyp.10082

Billi, P., Alemu, Y. T., & Ciampalini, R. (2015). Increased frequency of flash floods in Dire Dawa, Ethiopia: Change in rainfall intensity or human impact? Natural Quantiles, 76(2), 1373–1394. https://doi.org/10.1007/s11069-014-1554-0

Birundu, A. M., & Mutua, B. M. (2017). Analyzing the Mara River Basin Behaviour through Rainfall-Runoff Modeling. International Journal of Geosciences, 08(09), 1118–1132. https://doi.org/10.4236/ijg.2017.89064

Blöschl, G., Bierkens, M. F. P., Chambel, A., Cudennec, C., Destouni, G., Fiori, A., Kirchner, J. W., McDonnell, J. J., Savenije, H. H. G., Sivapalan, M., Stumpp, C., Toth, E., Volpi, E., Carr, G., Lupton, C., Salinas, J., Széles, B., Viglione, A., Aksoy, H., … Zhang, Y. (2019). Twenty-three unsolved problems in hydrology (UPH)–a community perspective. Hydrological Sciences Journal, 64(10), 1141–1158. https://doi.org/10.1080/02626667.2019.1620507

Bouffard, J.-S. (2014), A comparison of conceptual rainfall-runoff modelling structures and approaches for hydrologic prediction in ungauged peatland basins of the James Bay lowlands, Master's thesis, Carleton Univ., Ottawa, Ont.

Breuer, L., et al. (2009), Assessing the impact of land use change on hydrology by ensemble modeling (LUCHEM). I: Model intercomparison with current land use, Adv. Water Resour., 32(2), 129–146.

Byun, K., Chiu, C. M., & Hamlet, A. F. (2019). Effects of 21st century climate change on seasonal flow regimes and hydrologic extremes over the Midwest and Great Lakes region of the US. https://doi.org/10.1016/j.scitotenv.2018.09.063

Carter, R. Leemans, M. Lal, P. Whetton (2009.). Climate Scenario Development_TAR 13. Scenario. https://doi.org/10.1007/s13762-018-1797-4

Chaney, N. W., Sheffield, J., Villarini, G., & Wood, E. F. (2014). Development of a high-resolution gridded daily meteorological dataset over sub-Saharan Africa: Spatial analysis of trends in climate extremes. Journal of Climate, 27(15), 5815–5835. https://doi.org/10.1175/JCLI-D-13-00423.1

Charles, S., Chiew, F., Potter, N., Zheng, H., Fu, G., & Zhang, L. (2019). Impact of downscaled rainfall biases on projected runoff changes. Hydrology and Earth System Sciences Discussions, August, 1–29. https://doi.org/10.5194/hess-2019-375

Chen, J., Brissette, F. P., Chaumont, D., & Braun, M. (2013). Finding appropriate bias correction methods in downscaling precipitation for hydrologic impact studies over North America. Water Resources Research, 49(7), 4187–4205. https://doi.org/10.1002/wrcr.20331

Cheung, H., Gabriel, B., and Ashbindu, S. (2008). Trends and spatial distribution of annual and seasonal rainfall in Ethiopia. International Journal of Climatology.

Chu, X., Asce, A. M., & Steinman, A. (2009). Event and Continuous Hydrologic Modeling with HEC-HMS. 135(1), 119–124. https://doi.org/10.1061/(ASCE)0733-9437(2009)135

Collet, L., Beevers, L., & Prudhomme, C. (2017). Assessing the impact of climate change and extreme value uncertainty to extreme flows across Great Britain. Water (Switzerland), 9(2), 1–16. https://doi.org/10.3390/w9020103

Coulibaly, T., Islam, M., & Managi, S. (2020). The Impacts of Climate Change and Natural Disasters on Agriculture in African Countries.

Daba, M. H., & You, S. (2020). Assessment of climate change impacts on river flow regimes in the upstream of awash basin, ethiopia: Based on ipcc fifth assessment report (ar5) climate change scenarios. Hydrology, 7(4), 1–22. https://doi.org/10.3390/hydrology7040098

Dakhlaoui, H., Ruelland, D., Tramblay, Y., & Bargaoui, Z. (2017). Evaluating the robustness of conceptual rainfall-runoff models under climate variability in northern Tunisia. Journal of Hydrology, 550, 201–217. https://doi.org/10.1016/j.jhydrol.2017.04.032

Dale, A., Fant, C., Strzepek, K., Lickley, M., & Solomon, S. (2017). Climate model uncertainty in impact assessments for agriculture: A multi-ensemble case study on maize in sub Saharan Africa. Earth's Future, 5(3), 337–353. https://doi.org/10.1002/2017EF000539Das, T., Bardossy, A., Zehe, E., & He, Y. (2008). Comparison of conceptual model performance using different representations of spatial variability. 356(1e2), 106e118. J. Hydrol., 356(1-2), 106–118. https://doi.org/http://dx.doi.org/10.1016/j.jhydrol.2008.04.008

Deelstra, J., C. Farkas, A. Engebretsen, S. Kværnø, S. Beldring, A. Olszewska, and L. Nesheim (2010), Can we simulate runoff from agriculture dominated watersheds? Comparison of the DrainMod, SWAT, HBV, COUP and INCA models applied for the Skuterud catchment, Bioforsk FOKUS, 5(6), 119–128.

Demirel, M. C., M. J. Booij, and A. Y. Hoekstra (2015), The skill of seasonal ensemble low-flow forecasts in the Moselle River for three different hydrological models, Hydrol. Earth Syst. Sci., 19(1), 275–291.

Driessen, T. L. A., Hurkmansm, R. T. W. L., Terink, W., Hazenberg, P., Torfs, P. J. J. F. & Uijlenhoet, R. 2010 The hydrological response of the Ourthe catchment to climate change as modelled by the HBV model. Hydrology and Earth System Sciences 14, 651–665.

Edossa, D. C., Babel, M. S., and Gupta, A. D. (2010). Drought analysis in the Awash river basin, Ethiopia. Water Resour. Manag., 24, 1441–1460.

Eghdamirad, S., Johnson, F., Sharma, A., & Kim, J. H. (2019). The influence of dependence in characterizing multi-variable uncertainty for climate change impact assessments. Hydrological Sciences Journal, 64(6), 731–738. https://doi.org/10.1080/02626667.2019.1602777

Ehret, U., Zehe, E., Wulfmeyer, V., Warrach-Sagi, K., & Liebert, J. (2012). HESS Opinions "should we apply bias correction to global and regional climate model data?" Hydrology and Earth System Sciences, 16(9), 3391–3404. https://doi.org/10.5194/hess-16-3391-2012

Ertugrul, M. (2019). Future Forest Fire Danger Projections Using Global Circulation Models (GCM) in Turkey. Fresenius Environmental Bulletin, 28(April), 3261–3269.

Fan, X., Duan, Q., Shen, C., Wu, Y., & Xing, C. (2020). Global surface air temperatures in CMIP6: Historical performance and future changes. Environmental Research Letters, 15(10). https://doi.org/10.1088/1748-9326/abb051

Farzaneh, M. R., Eslamian, S., Samadi, S. Z., & Akbarpour, A. (2012). An appropriate general circulation model (GCM) to investigate climate change impact. International Journal of HydrologyScienceand Technology, 2(1), 34–47. https://doi.org/10.1504/IJHST.2012.045938

Flato, G., Marotzke, B., Abiodun, P., Braconnot, S., Chou, W., Collis, P., Cox, F., Driouech, S., Emori, V., Eyring, C., Forest, P., Gleckler, E., Guilyardi, C., Jakob, V., Kattsov, C., and Rummukainen. M. (2017). Evaluation of climate models. The Physical Science Basis. Contribution of working group 1 to the fifth assessment report of the intergovernmental panel on climate change. Cambridge University Press, Cambridge, United Kingdom and New York, NY, USA.

Fowler, H. J., Ekström, M., Blenkinsop, S., & Smith, A. P. (2007). Estimating change in extreme European precipitation using a multimodel ensemble. Journal of Geophysical Research Atmospheres, 112(18). https://doi.org/10.1029/2007JD008619

Gao, C., Booij, M., & Xu, Y.-P. (2020). Assessment of extreme flows and uncertainty under climate change: disentangling the contribution of RCPs, GCMs and internal climate variability. Hydrology and Earth System Sciences Discussions, February, 1–28. https://doi.org/10.5194/hess-2020-25

Getahun, Y., and Lanen, H. (2018). Impact of Climate Change on Hydrology of the Upper Awash River Basin (Ethiopia): Inter-comparison of old SRES and new RCP scenarios. https://www.researchgate.net/publication/316505332.

Giorgi, F., & GAO, X. J. (2018). Regional earth system modeling: review and future directions. AtmosphericandOceanicScienceLetters,11(2),189–197.

Griffis, V. W., & Stedinger, J. R. (2007). Evolution of Flood Frequency Analysis with Bulletin 17. June, 283–297.

Gudmundsson, L., Wagener, T., Tallaksen, L. M., & Engeland, K. (2012). Evaluation of nine large-scale hydrological models with respect to the seasonal runoff climatology in Europe. Water Resources Research, 48(11). https://doi.org/10.1029/2011WR010911

Gutjahr, O., & Heinemann, G. (2013). Comparing precipitation bias correction methods for high-resolution regional climate simulations using COSMO-CLM: Effects on extreme values and climate change signal. Theoretical and Applied Climatology, 114(3–4), 511–529. https://doi.org/10.1007/s00704-013-0834-z

Haile, A.T., Tefera, F.T. and Rientjes, T. (2016). Flood forecasting in Upper Awash River basin using satellite and quantitative precipitation forecast data. International Journal of Applied Earth Observation and Geoinformation, 475-484.

Hamon, W. R. (1964). Computation of direct runoff amounts from storm rainfall. In General Assembly of Berkeley, Symposium on Surface Waters: Vol. Extract of (pp. 52–62).

Hassan, R. (2006). Climate change and African agricultures, Policy Note. Human Development Report, 2007/2008. Climate Change and Human Development in Africa: Assessing the Risks

and Vulnerability of Climate Change in Kenya, Malawi and Ethiopia. By IGAD Climate Prediction and Applications Centre (ICPAC).

Hattermann, F. F., Vetter, T., Breuer, L., Su, B., Daggupati, P., Donnelly, C., Fekete, B., Florke, F., Gosling, S. N., Hoffmann, P., Liersch, S., Masaki, Y., Motovilov, Y., Muller, C., Samaniego, L., Stacke, T., Wada, Y., Yang, T., & Krysnaova, V. (2018). Sources of uncertainty in hydrological climate impact assessment: A cross-scale study. Environmental Research Letters, 13(1). https://doi.org/10.1088/1748-9326/aa9938

He, Y., Wetterhall, F., Bao, H. J., Cloke, H. l., Li, Z., Pappenberger, F., and Hu, Y. (2018). Ensemble forecasting using TIGGE for the July–September 2008 floods in the upper Huai catchment: a case study. Atmos. Sci. Lett., 11, 132–138. https://doi.org/10.1002/asl.270.

Her, Y., Yoo, S. H., Cho, J., Hwang, S., Jeong, J., & Seong, C. (2019). Uncertainty in hydrological analysis of climate change: multi-parameter vs. multi-GCM ensemble predictions. Scientific Reports, 9(1), 1–22. https://doi.org/10.1038/s41598-019-41334-7

Hyeder. A ,Sherman .R & Dirk .W (2009).Climate change and Ethiopia. 6 (2009) 322009. 6(February), 9–10. https://doi.org/10.1088/1755-1307/6/2/322009

IHMS: Integrated Hydrological Modelling System. Manual, Version4.5. Swedish Meteorological and Hydrological Institute, Norrkoping, Sweden, 1999.

IPCC (Intergovernmental Panel on Climate Change). 2001: The Scientific Basis. Contribution of Working Group I to the Third Assessment Report of the Intergovernmental Panel on Climate Change

IPCC (Intergovernmental Panel on Climate Change). (2007). Climate change: AR4 synthesis report, Cambridge University Press, Cambridge.

IPCC (Intergovernmental Panel on Climate Change). (2013). Climate Change: The Physical Science Basis. Contribution of Working Group I to the Fifth Assessment Report of the Intergovernmental Panel on Climate Change

IPCC (Intergovernmental Panel on Climate Change). (2014). the Scientific Basis. Contribution of Working Group I to the Third Assessment Report of the Intergovernmental Panel on Climate Change

Joseph, J., Ghosh, S., Pathak, A., & Sahai, A. K. (2018b). Hydrologic impacts of climate change: Comparisons between hydrological parameter uncertainty and climate model uncertainty. Journal of Hydrology, 566(September), 1–22. https://doi.org/10.1016/j.jhydrol.2018.08.080

Kalita, A., Bormudoi, A., & Saikia, M. Das. (2019). Probability Distribution of Rainfall and Discharge of Kulsi River Basin. (April). https://doi.org/10.14445/23488352/IJCE-V4I5P107

Kay, A. L., Davies, H. N., Bell, V. A., & Jones, R. G. (2009). Comparison of uncertainty sources for climate change impacts: Flood frequency in England. Climatic Change, 92(1–2), 41–63. https://doi.org/10.1007/s10584-008-9471-4

Keast, D., & Ellison, J. (2013). Magnitude frequency analysis of small floods using the annual and partial series. Water (Switzerland), 5(4), 1816–1829. https://doi.org/10.3390/w5041816

Kingston, D. G., Thompson, J. R., & Kite, G. (2011). Uncertainty in climate change projections of discharge for the Mekong River Basin. Hydrology and Earth System Sciences, 15(5), 1459–1471. https://doi.org/10.5194/hess-15-1459-2011

Knutti, R., & Sedláček, J. (2013). Robustness and uncertainties in the new CMIP5 climate model projections. Nature Climate Change, 3(4), 369–373. https://doi.org/10.1038/nclimate1716

Kobold, M., Brilly, M., Kobold, M., The, M. B., & Quantiles, N. (2006). The use of HBV model for flash flood forecasting To cite this version : HAL Id : hal-00299304 The use of HBV model for flash flood forecasting. 6(3).

Krinner, G., & Flanner, M. G. (2018). Striking stationarity of large-scale climate model bias patterns under strong climate change. Proceedings of the National Academy of Sciences of the United States of America, 115(38), 9462–9466. https://doi.org/10.1073/pnas.1807912115

Lafon, T., Dadson, S., Buys, G., & Prudhomme, C. (2013). Bias correction of daily precipitation simulated by a regional climate model: A comparison of methods. International Journal of Climatology, 33(6), 1367–1381. https://doi.org/10.1002/joc.3518

Lawrence, D. (2020). Uncertainty introduced by flood frequency analysis in projections for changes in flood magnitudes under a future climate in Norway. Journal of Hydrology: Regional Studies, 28(December 2019), 100675. https://doi.org/10.1016/j.ejrh.2020.100675

Lindström, G., Johansson, B., Persson, M., Gardelin, M., & Bergström, S. (1997). Development and test of the distributed HBV-96 hydrological model. Journal of Hydrology, 201(1), 272-288.

https://doi.org/10.1016/S0022-1694(97)00041-3

Liou, Y. A., & Mulualem, G. M. (2019). Spatio-temporal assessment of drought in Ethiopia and the impact of recent intense droughts. Remote Sensing, 11(15). https://doi.org/10.3390/rs11151828

Luhunga, P. M., Kijazi, A. L., Chang'a, L., Ng'ongolo, H., Kondowe, A., Magnusson, L. Services, H. (2015). Valuing Weather and Climate : In World Meteorological Organization (Vol. 09). https://doi.org/10.4236/acs.2019.92014

Mader,S.(2019).Whatdrivesclimatechange .UniversityofBern(August).https://doi.org/10.13140/RG.2.2.13792.23045

Mamo, S., Berhanu, B., & Melesse, A. M. (2019). Historical flood events and hydrological extremes in Ethiopia. (September) Ministry of Water, Irrigation and Energy/GIRDC/ENTRO,AddisAbaba,Ethiopiahttps://www.researchgate.net/publication/33502

Mendez, M., Maathuis, B., Hein-Griggs, D., & Alvarado-Gamboa, L. F. (2020). Performance evaluation of bias correction methods for climate change monthly precipitation projections over Costa Rica. Water (Switzerland), 12(2). https://doi.org/10.3390/w12020482

Meenu, R., Rehana, S., & Mujumdar, P. P. (2013). Assessment of hydrologic impacts of climate change in Tunga – Bhadra river basin , India with HEC-HMS and SDSM. 1589(May 2012), 1572–1589. https://doi.org/10.1002/hyp.9220

Meresa, Hadush K Romanowicz, R. J., Bogdanowicz, E., Debele, S. E., Doroszkiewicz, J., Hisdal, H., Lawrence, D., Wong, W. K. (2016). Climate Change Impact on Hydrological Extremes: Preliminary Results from the Polish-Norwegian Project. Acta Geophysica, 64(2), 477–509. https://doi.org/10.1515/acgeo-2016-0009

Meresa, H. (2019). Modelling of river flow in ungauged catchment using remote sensing data: application of the empirical (SCS-CN), Artificial Neural Network (ANN) and Hydrological Meresa, Hadush K., & Romanowicz, R. J. (2017). The critical role of uncertainty in projections of hydrological extremes. Hydrology and Earth System Sciences. https://doi.org/10.5194/hess-21-4245-2017

Meresa, Hadush K., & Gatachew, M. T. (2018). Climate change impact on river flow extremes in the Upper Blue Nile River basin. Journal of Water and Climate Change, (November), jwc2018154. https://doi.org/10.2166/wcc.2018.154

Meresa, Hadush K., & Gatachew, M. T. (2019). Climate change impact on river flow extremes in the upper blue nile river basin. Journal of Water and Climate Change, 10(4), 759–781. https://doi.org/10.2166/wcc.2018.154

Meresa, Hadush Kidane. (2019). River flow characteristics and changes under the influence of varyingclimateconditions. https://doi.org/10.1111/nrm.12242

NMA, (2001). Initial National Communication of Ethiopia to the United Nations Framework Convention on Climate Change, Addis Ababa: NMSA.

Osman, Y., Al-Ansari, N., & Abdellatif, M. (2019). Climate change model as a decision support tool for water resources management in northern Iraq: A case study of Greater Zab River. Journal of Water and Climate Change, 10(1), 197–209. https://doi.org/10.2166/wcc.2017.083

Osuch, M., Lawrence, D., Meresa, H. K., Napiorkowski, J. J., & Romanowicz, R. J. (2017).Projected changes in flood indices in selected catchments in Poland in the 21st century. Stochastic Environmental Research and Risk Assessment, 31(9). https://doi.org/10.1007/s00477-016-1296-5

Pechlivanidis, I. G., Arheimer, B., Donnelly, C., Hundecha, Y., Huang, S., Aich, V., Samaniego, L., Eisner, S., & Shi, P. (2017). Analysis of hydrological extremes at different hydro-climatic regimes under present and future conditions. Climatic Change, 141(3), 467–481. https://doi.org/10.1007/s10584-016-1723-0

Piani, C., Haerter, J. O., & Coppola, E. (2010). Statistical bias correction for daily precipitation in regional climate models over Europe. Theoretical and Applied Climatology, 99(1–2), 187–192. https://doi.org/10.1007/s00704-009-0134-9

Pierce, D. W., Cayan, D. R., Maurer, E. P., Abatzoglou, J. T., & Hegewisch, K. C. (2015). Improved bias correction techniques for hydrological simulations of climate change. Journal of Hydrometeorology, 16(6), 2421–2442. https://doi.org/10.1175/JHM-D-14-0236.1

Plesca, I., E. Timbe, J. F. Exbrayat, D. Windhorst, P. Kraft, P. Crespo, K. B. Vachea, H. G. Frede, and L. Breuer (2012), Model intercomparison to explore catchment functioning: Results from a remote montane tropical rainforest, Ecol. Modell., 239, 3–13.

Projected changes in flood indices in selected catchments in Poland in the 21st century. Stochastic Environmental Research and Risk Assessment, 31(9). https://doi.org/10.1007/s00477-016-1296-5.

Putty, M. R. Y., & Prasad, R. (2000). Understanding runoff processes using a watershed model a case study in the Western Ghats in South India. 228, 215–227.

Refsgaard, J. C., Drews, M., Jeppesen, E., Madsen, H., Markandya, A., Olesen, J. E., Porter, J. R., & Christensen, J. H. (2013). The role of uncertainty in climate change adaptation strategies A Danish water management example. 337–359. https://doi.org/10.1007/s11027-012-9366-6.

Roth, V., Lemann, T., Zeleke, G., & Teklay, A. (2018). Effects of climate change on water resources in the upper Blue Nile Basin of Ethiopia. Heliyon, November 2017. https://doi.org/10.1016/j.heliyon.2018.e00771.

Rojas, R., Feyen, L., & Watkiss, P. (2013). Climate change and river floods in the European Union: Socio-economic consequences and the costs and benefits of adaptation. Global Environmental Change, 23(6), 1737–1751. https://doi.org/10.1016/j.gloenvcha.2013.08.006.

Saini, R., Wang, G., Yu, M., & Kim, J. (2015). Phytoplankton light absorption and the package effect in relation to photosynthetic and photoprotective pigments in the northern tip of Antarctic Peninsula. Journal of Geophical Research, 3679–3699. https://doi.org/10.1002/2014JD022599.

Samani, Z. (2000). Estimating Solar Radiation and Evapotranspiration Using Minimum Climatological Data. Journal of Irrigation and Drainage Engineering, 126(4), 265- 267267. https://doi.org/10.1061/(ASCE)0733-9437(2000)126:4(265).

Serdeczny, O., Adams, S., Coumou, D., Hare, W., & Perrette, M. (2016). repercussions. JANUARY. https://doi.org/10.1007/s10113-015-0910-2.

Simane, B., Beyene, H., Deressa, D., Kumie, A., Berhane, K., and Samet, J. (2016). Review of Climate Change and Health in Ethiopia: Status and Gap Analysis. Ethiop J Health Dev, 30, 28.

Shawul, A. A., Chakma, S., & Melesse, A. M. (2019). Journal of Hydrology : Regional Studies The response of water balance components to land cover change based on hydrologic modeling and partial least squares regression (PLSR) analysis in the Upper Awash Basin. Journal of Hydrology:RegionalStudies,26(October),100640.https://doi.org/10.1016/j.ejrh.2019.

Steele-Dunne, S., P. Lynch, R. McGrath, T. Semmler, S. Wang, J. Hanafin, and P. Nolan (2008), The impacts of climate change on hydrology in Ireland, J. Hydrol., 356(1–2), 28–45.

Stern, D. I., & Kaufmann, R. K. (2014). Anthropogenic and natural causes of climate change Anthropogenic and natural causes of climate change. (January). https://doi.org/10.1007/s10584-013-1007-x

Taddese, G., Sonder, K., and Peden, D. (2006). The Water of Awash River Basin a Future Challange to Ethiopia. International Live Stock Research Institute (ILRI).

Tarekegn, T. H. (2012). Two Dimension Hydrodaynamic Modeling of Flooding using ASTER DEM in Ribb Catchment, Ethiopia. Journal of Applied Earth Observationand Geo Information.

Tarekegn D, Tadege A. 2006. Assessing the Impact of Climate Change onthe Water Resources of the Lake Tana Basin Using the Watbal Model.CEEPA, University of Pretoria: Sweden; 15.

Taye, M. T., Willems, P., & Block, P. (2015). Implications of climate change on hydrological extremes in the Blue Nile basin: A review. Journal of Hydrology: Regional Studies, 4, 280–293. https://doi.org/10.1016/j.ejrh.2015.07.001

Telinde, A. H., J. C. J. H. Aerts, R. T. W. L. Hurkmans, and M. Eberle (2008), Comparing model performance of two rainfall-runoff models in the Rhine Basin using different atmospheric forcing data sets, Hydrol. Earth Syst. Sci., 12(3), 943–957

Temesgen, T. (2000). Drought and its predictability in Ethiopia. https://doi.org/10.1007/s10584-013-1007-x

Teng, J., Vaze, J., Chiew, F. H. S., Wang, B., & Perraud, J. M. (2012). Estimating the relative uncertainties sourced from GCMs and hydrological models in modeling climate change impact on runoff. Journal of Hydrometeorology, 13(1), 122–139. https://doi.org/10.1175/JHM-D-11-058.1

Terink, W., Hurkmans, R., Torfs, P., and Uijlenhoet, R. (2009). Evaluation of a bias correction method applied to downscaled precipitation and temperature reanalysis data for Rhine Basins. Journal of Hydrology Earth System Science, 6, 5377-5413.

Teutschbein, C., & Seibert, J. (2010). Regional climate models for hydrological impact studies at the catchment scale: A review of recent modeling strategies. Geography Compass, 4(7), 834–860. https://doi.org/10.1111/j.1749-8198.2010.00357.

Teutschbein, C., & Seibert, J. (2013). Is bias correction of regional climate model (RCM) simulations possible for non-stationary conditions. Hydrology and Earth System Sciences, 17(12), 5061–5077. https://doi.org/10.5194/hess-17-5061-2013

Thober, S., Kumar, R., Wanders, N., Marx, A., Pan, M., Rakovec, O., Samaniego, L., Sheffield, J., Wood, E. F., & Zink, M. (2018). Multi-model ensemble projections of European river floods and high flows at 1.5, 2, and 3 degrees global warming. Environmental Research Letters, 13(1). https://doi.org/10.1088/1748-9326/aa9e35

Unduche, F., Tolossa, H., Senbeta, D., & Zhu, E. (2018). Evaluation of four hydrological models for operational flood forecasting in a Canadian Prairie watershed. Hydrological Sciences Journal, 63(8), 1133–1149. https://doi.org/10.1080/02626667.2018.1474219.

Vetter, T., S. Huang, V. Aich, T. Yang, X. Wang, V. Krysanova, and F. Hattermann (2015), Multi-model climate impact assessment and intercomparison for three large-scale river basins on three continents, Earth Syst. Dyn., 6(1), 17–43.

Wang, H.-M., Chen, J., Xu, C.-Y., Chen, H., Guo, S., Xie, P., & Li, X. (2019). Does the weighting of climate simulations result in a more reasonable quantification of hydrological impacts? Hydrology and Earth System Sciences Discussions, February, 1–29. https://doi.org/10.5194/hess-2019-24.

Wilby, L. R., Zorita, E., Timbal, B., Whetton, P., Mearns, L. O. & Charles, S. P. (2004). Guidelines for use of Climate Scenario Developed from Statistical Downscaling Methods. Environmental Agency of England and Wales, UK.

Woldemeskel, F. M., Sharma, A., Sivakumar, B., & Mehrotra, R. (2014). A framework to quantify GCM uncertainties for use in impact assessment studies. Journal of Hydrology, 519(PB), 1453–1465. https://doi.org/10.1016/j.jhydrol.2014.09.025.

Yan, D., Werners, S. E., Ludwig, F., & Huang, H. Q. (2015). Hydrological response to climate change: The Pearl River, China under different RCP scenarios. Journal of Hydrology: Regional Studies, 4(PB), 228–245. https://doi.org/10.1016/j.ejrh.2015.06.006.

Yang, W., Andréasson, J., Graham, L. P., Olsson, J., Rosberg, J., & Wetterhall, F. (2010). Distribution-based scaling to improve usability of regional climate model projections for hydrological climate change impacts studies. Hydrology Research, 41(3–4), 211–229. https://doi.org/10.2166/nh.2010.004.

Zhang, X., and G. Lindstr€om (1996), A comparative study of a Swedish and a Chinese hydrological model, J. Am. Water Resour. Assoc., 32(5),985–994.

Zhang, Q., Tang, Q., Knowles, J. F., & Livneh, B. (2019). Contribution of model parameter uncertainty to future hydrological projections. Hydrology and Earth System Sciences Discussions, February, 1–31. https://doi.org/10.5194/hess-2019-52.

APPENDICES

Appendices - A1: Filling in missed rainfall and temperature data

Normal ratio method can be defined by

$$Px = \frac{Nx}{N}\left(\frac{P1}{N1} + \frac{P2}{N2} + \frac{P3}{N3} \ldots + \frac{Pn}{Nn}\right) \ldots\ldots\ldots\ldots\ldots\ldots\ldots\ldots\ldots\ldots \text{A1}$$

Where, Px =Missing value of rainfall (RF) to be computed.

Nx = Normal annual rainfall for the station in question for recording period.

N1, N2………Nn = Normal annual rainfall for the neighboring station.

P1, P2. .... Pn = Rainfall of neighboring station on missing period

N = Number of stations used in the computation.

Arithmetic mean method defined by:

$$Px = \frac{1}{n}\sum_{i=1}^{n} Pi \ldots\ldots\ldots\ldots\ldots\ldots\ldots\ldots\ldots\ldots\ldots\ldots \text{A2}$$

Where: Px = missing station rainfall

Pi = rainfall at the i^{th} station

N = is the number of nearby stations

Appendices - A2: Rainfall data-set consistency test methodology

The slope correction equation is defined by the following formula:

Pcx = Px $\frac{Mc}{Ma}$ ……..A3

Where: Pcx = corrected RF at any time period T1 at station x

Px = Original recorded RF at time period T1 at station x

Mc = Corrected slope of the double mass curve

Ma = Original slope of the double mass curve